IMMUNOLOGY

Severe hematotoxicity after CD19 CAR-T therapy is associated with suppressive immune dysregulation and limited CAR-T expansion

Kai Rejeski[1,2,3,4]*, Ariel Perez[5,6], Gloria Iacoboni[7,8], Viktoria Blumenberg[1,2,3,4], Veit L. Bücklein[1,2,3,4], Simon Völkl[4,9], Olaf Penack[3,10], Omar Albanyan[5,11], Sophia Stock[1,3], Fabian Müller[4,9], Philipp Karschnia[12], Agnese Petrera[13], Kayla Reid[5], Rawan Faramand[5], Marco L. Davila[5], Karnav Modi[5], Erin A. Dean[14], Christina Bachmeier[5], Michael von Bergwelt-Baildon[1,3,4], Frederick L Locke[5], Wolfgang Bethge[15], Lars Bullinger[3,10], Andreas Mackensen[4,9], Pere Barba[7,8], Michael D. Jain[5]*†, Marion Subklewe[1,2,3,4]*†

Prolonged cytopenias after chimeric antigen receptor (CAR) T cell therapy are a significant clinical problem and the underlying pathophysiology remains poorly understood. Here, we investigated how (CAR) T cell expansion dynamics and serum proteomics affect neutrophil recovery phenotypes after CD19-directed CAR T cell therapy. Survival favored patients with "intermittent" neutrophil recovery (e.g., recurrent neutrophil dips) compared to either "quick" or "aplastic" recovery. While intermittent patients displayed increased CAR T cell expansion, aplastic patients exhibited an unfavorable relationship between expansion and tumor burden. Proteomics of patient serum collected at baseline and in the first month after CAR-T therapy revealed higher markers of endothelial dysfunction, inflammatory cytokines, macrophage activation, and T cell suppression in the aplastic phenotype group. Prolonged neutrophil aplasia thus occurs in patients with systemic immune dysregulation at baseline with subsequently impaired CAR-T expansion and myeloid-related inflammatory changes. The association between neutrophil recovery and survival outcomes highlights critical interactions between host hematopoiesis and the immune state stimulated by CAR-T infusion.

INTRODUCTION

CD19-directed CAR T cell therapy (CD19.CAR-T) has substantially improved treatment outcomes for multiple refractory B cell malignancies (*1*–*6*). However, this practice-changing immunotherapy platform is accompanied by a unique toxicity profile, which typically includes cytokine release syndrome (CRS) and immune effector cell-associated neurotoxicity syndrome (ICANS) (*7*, *8*). Real-world evidence has further highlighted the role of hematological toxicity, which represents the most frequently encountered grade ≥ 3 toxicity after CD19.CART (*9*, *10*). Profound and prolonged neutropenia can predispose for severe infectious complications, which drive nonrelapse mortality after CAR-T therapy (*11*–*15*) (see "note added in proof").

The recently termed Immune Effector Cell-Associated Hematotoxicity (ICAHT) (see "note added in proof") usually presents as an acute drop in peripheral blood counts due to the lymphodepleting chemotherapy administered before CAR-T therapy (most commonly fludarabine and cyclophosphamide). In some cases, the cytopenias are prolonged in nature, often persisting long after lymphodepletion and resolution of acute CAR-T toxicities (CRS and ICANS). Neutrophil recovery after CAR T cell therapy is typically characterized by a biphasic pattern with intermittent recovery followed by a second dip, or even multiple dips (*10*, *16*). Furthermore, clinically challenging cases of profound granulocyte colony-stimulating factor (G-CSF) refractory aplasia have been reported, which can ultimately necessitate the application of a stem cell boost from either an autologous or allogeneic source (*12*, *17*–*22*). To account for these qualitative cytopenia differences, we recently proposed a novel classification system for CAR-T–related hematotoxicity, defining three unique phenotypes of neutrophil recovery: quick versus intermittent versus aplastic (*10*).

Overall, the pathomechanistic basis of hematological toxicity remains ill-defined and incompletely understood. While chemotherapy undoubtedly contributes to cytopenias, it does not alone explain the observed clinical patterns of cytopenias after CAR T cell therapy, and the delayed onset suggests that the mechanism is likely due to a CAR T cell–related impact on (healthy)

[1]Department of Medicine III – Hematology/Oncology, University Hospital, LMU Munich, Munich, Germany. [2]Laboratory for Translational Cancer Immunology, LMU Gene Center, Munich, Germany. [3]German Cancer Consortium (DKTK), Munich and Berlin sites, and German Cancer Research Center, Heidelberg, Germany. [4]Bavarian Cancer Research Center (BZKF), partner sites, Munich and Erlangen, Germany. [5]Department of Blood and Marrow Transplant and Cellular Immunotherapy, Moffitt Cancer Center, Tampa, FL, USA. [6]Blood and Marrow Transplant Program, Miami Cancer Institute, Miami, FL, USA. [7]Department of Hematology, University Hospital Vall d'Hebron, Vall d'Hebron Institute of Oncology (VHIO), Barcelona, Spain. [8]Department of Medicine, Universitat Autònoma de Barcelona, Bellaterra, Spain. [9]Department of Internal Medicine 5, Hematology and Oncology, Friedrich-Alexander-Universität Erlangen-Nürnberg and University Hospital Erlangen, Erlangen, Germany. [10]Department of Hematology, Oncology and Tumorimmunology, Charité Universitätsmedizin Berlin, corporate member of Freie Universität Berlin und Humboldt-Universität zu Berlin, Berlin, Germany. [11]Adult Hematology-Oncology and Stem Cell Transplantation, King Fahad Specialist Hospital, Dammam, Saudi Arabia. [12]Department of Neurosurgery, University Hospital, LMU Munich, Munich, Germany. [13]Metabolomics and Proteomics Core Facility, Helmholtz Zentrum Munich – German Research Center for Environmental Health, Munich, Germany. [14]Division of Hematology and Oncology, Department of Medicine, University of Florida, Gainesville, FL, USA. [15]Department of Hematology, Oncology, Immunology and Rheumatology, University Hospital Tübingen, Tübingen, Germany.
*Corresponding author. Email: kai.rejeski@med.uni-muenchen.de (K.Rej.); michael.jain@moffitt.org (M.D.J.); marion.subklewe@med.uni-muenchen.de (M.S.)
†These authors contributed equally to this work.

hematopoiesis (*23*). Furthermore, the success of stem cell boost as a therapeutic strategy suggests that the hematologic injury is not ongoing or autoimmune in nature (*20*, *21*). Previous studies have linked severe CRS and elevated CRS-related cytokine levels to more pronounced cytopenias (*24*). However, not all patients with severe CRS develop hematological toxicity and subsequent dips in neutrophil counts occur after CRS has resolved.

In previous work, we observed that both pre–CAR-T bone marrow (BM) reserve (e.g., baseline cytopenias) and inflammatory state [e.g., C-reactive protein (CRP) and ferritin] are associated with prolonged neutropenia (*10*, *13*). Still, it remained unclear in what manner these baseline findings relate to CAR T cell expansion and persistence upon infusion. Moreover, the precise systemic inflammatory stressors mediating hematotoxicity are poorly characterized. Here, we therefore aimed to understand the mechanisms underlying prolonged neutropenia after CAR-T therapy. Utilizing the established neutrophil recovery phenotypes as a blueprint of hematological toxicity, we analyzed their influence on clinical outcomes and coincident toxicity and their relation to CAR-T expansion and serum proteomics.

RESULTS

Baseline patient characteristics by neutrophil recovery phenotype

In this multicenter retrospective study, CAR-T–related toxicity and clinical outcomes were analyzed in a representative cohort of relapsed and/or refractory large B cell lymphoma (R/R LBCL) patients treated in a real-world setting (Fig. 1A). Median age was 64 (range, 19 to 83) years, median Eastern Cooperative Oncology Group (ECOG) was 1 [interquartile range (IQR), 0 to 1], and median International Prognostic Index (IPI) was 3 (IQR, 2 to 4) (Table 1). Patients received a median of three prior treatment lines (excluding bridging therapy), including 26% with a prior autologous stem cell transplantation. A total of 262 patients (76%) received bridging therapy, which was most commonly chemotherapy-based (64%), followed by radiation therapy (13%). Transformed lymphoma was noted in 79 patients (23%), while BM infiltration of the underlying lymphoma was observed in 16% of cases.

The overall distribution of neutrophil recovery phenotypes was 40, 42, and 18% (Q versus I versus A) (Fig. 1B). In terms of baseline characteristics, "aplastic" patients displayed a higher ECOG (median, 1; IQR, 1 to 2) and increased serum lactate dehydrogenase (LDH) levels (Q versus I versus A: median, 254 versus 266 versus 298 U/liter, $P = 0.04$) at lymphodepletion compared to the other phenotypes (Table 1). Bridging therapy was more frequently used in the aplastic group (Q versus I versus A: 71% versus 74% versus 91%, $P < 0.001$), including the common application of chemotherapy-based bridging strategies (Q versus I versus A: 54% versus 64% versus 81%, $P = 0.05$). Furthermore, aplastic patients more commonly exhibited BM infiltration (Q versus I versus A: 10% versus 15% versus 31%, $P = 0.002$) and double/triple expressor status on histological examination (40% versus 36% versus 57%, $P = 0.02$). On the other hand, age and absolute lymphocyte count did not significantly differ by phenotype. Notably, patients who developed the aplastic phenotype presented with significantly higher levels of the systemic inflammatory markers CRP (Q versus I versus A: median 1.0 versus 0.9 versus 2.8 mg/dl, $P < 0.001$) and ferritin (median 381 versus 493 versus 1110 ng/ml, $P < 0.001$) at lymphodepletion compared to their "quick" and "intermittent" counterparts. They also observed significantly impaired hematopoietic function including lower absolute neutrophil count (ANC) (Q versus I versus A: 3320 versus 2380 versus 1410 per μl, $P < 0.001$), platelet count (174 versus 162 versus 107 G/liter, $P < 0.001$), and hemoglobin (10.7 versus 10.3 versus 9.1 g/dl, $P < 0.001$). This translated to significantly increased CAR-HEMATOTOX scores in the aplastic patients compared to the other phenotypes (Q versus I versus A: median 1 versus 1 versus 3, $P < 0.001$); however, no significant difference was noted when directly comparing the quick and intermittent groups ($P = 0.38$).

Influence of neutrophil recovery phenotypes on CAR-T–related toxicity and nonrelapse mortality

When studying the duration of CAR-T–related neutropenia, we found that aplastic patients exhibited the longest median duration of severe neutropenia (Q versus I versus A: 5.5 versus 9 versus 26 days, $P < 0.001$, Fig. 1C). Concomitantly, supportive measures for prolonged cytopenia were more commonly utilized in the aplastic patients, especially TPO agonists (Q versus I versus A: 0% versus 1% versus 8%, $P < 0.001$) and stem cell boosts (Q versus I versus A: 0% versus 0% versus 8%, $P < 0.001$) (table S1). Conversely, G-CSF was only rarely applied in the patients with quick recovery (Q versus I versus A: 11% versus 70% versus 70%, $P < 0.001$). While we did not observe a significant difference in the duration of severe neutropenia by CAR product (fig. S1A), patients treated with axicabtagene ciloleucel (Axi-cel) more frequently displayed biphasic neutrophil recovery [intermittent phenotype, Axi-cel versus tisagenlecleucel (Tisa-cel): 47% versus 34%, $P = 0.018$, fig. S1B].

The extended duration of severe neutropenia translated into a higher rate of any-grade (Q versus I versus A: 39% versus 49% versus 64%, $P = 0.002$) and particularly severe infections (16% versus 22% versus 44%, $P < 0.001$) in the aplastic cohort (Fig. 1D), including five life-threatening (8%) and five fatal infections (8%) (table S2). Bacterial infections represented the most commonly identified pathogen, accounting for 52% of severe infections (fig. S2A). The rate of severe bacterial infections was significantly higher in the aplastic group (Q versus I versus A: 7% versus 14% versus 28%, $P < 0.001$, fig. S2B). Both the aplastic and intermittent patients more commonly received broad-spectrum intravenous antibiotics such as piperacillin/tazobactam or carbapenems, during the first 10 days after CAR T cell infusion (table S2). On the other hand, fluoroquinolone-based antibiotic prophylaxis was less frequently applied as a supportive measure in the intermittent group.

The rate of severe CRS did not significantly differ by neutrophil recovery phenotype (Q versus I versus A: 8% versus 9% versus 13%, $P = 0.22$, Fig. 1E and table S3). However, severe ICANS was less frequently observed in the quick cohort (Q versus I versus A: 9% versus 20% versus 23%, $P = 0.002$, Fig. 1F and table S3). As a result, supportive measures including tocilizumab, anakinra, and high-dose corticosteroids were less commonly administered in the quick patients. Of interest, a significantly increased percentage of patients with aplastic neutrophil recovery required an intensive care unit (ICU) admission for the management of CAR-T–related toxicity (Q versus I versus A: 12% versus 13% versus 25%, $P = 0.02$, table S3). Furthermore, we noted a trend toward increased 1-year nonrelapse mortality in the aplastic patients (1-year NRM: 3.5% versus 5% versus 9%, $P = 0.18$, Fig. 1G). Notably, the quick phenotype was associated with shortened hospital stays compared to the other

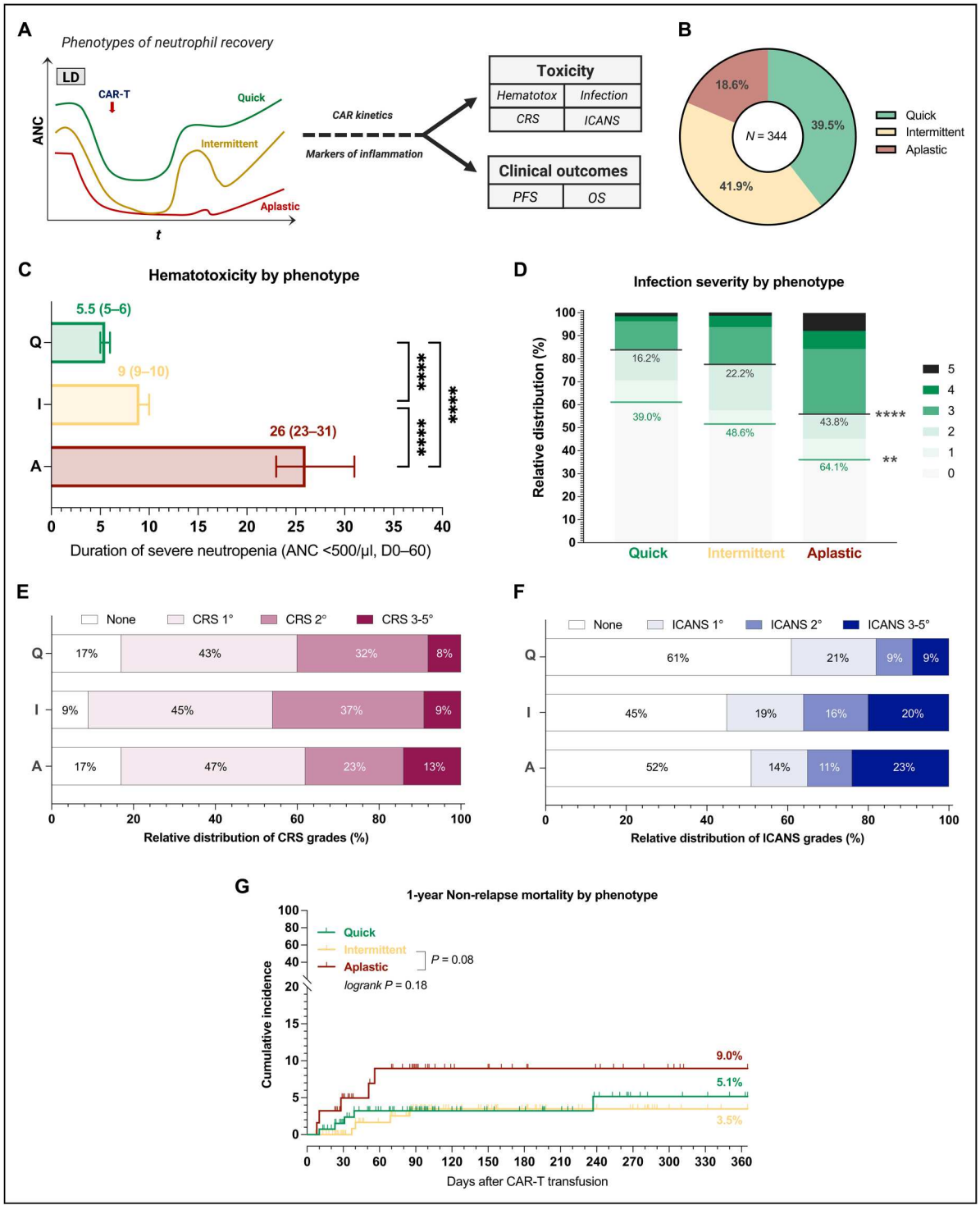

Fig. 1. Influence of phenotypes of neutrophil recovery on CAR-T–related toxicity and nonrelapse mortality. (**A**) Schema of study design on the basis of neutrophil recovery phenotypes: quick recovery (green) versus intermittent recovery (yellow) versus aplastic (red). (**B**) Overall distribution of neutrophil recovery phenotypes. (**C**) Cumulative duration of severe neutropenia (ANC <500/µl) between day 0 and day +60 by phenotype. *P* value determined by Kruskal-Wallis test and Dunn's multiple comparison test. (**D**) Relative distribution of infection grades by phenotype (all infection subtypes). Infection grades (1° to 5°) are color-coded in shades of green with the connecting green and gray lines and percentage numbers comparing all-grade and grade ≥ 3 infections by phenotype [infection grading: Rejeski *et al.* (*13*)]. *P* value determined by chi-squared test (**$P < 0.01$ and ****$P < 0.0001$). (**E** and **F**) Relative distribution of CRS grades (E) and ICANS grades (F) according to ASTCT criteria by phenotype. (**G**) One-year nonrelapse mortality (NRM) in patients with quick (green) and intermittent (yellow) versus aplastic (red) neutrophil recovery. The *P* value of the Mantel-Cox log-rank test comparing phenotype groups and for the direct comparison of intermittent versus aplastic is depicted. ANC, absolute neutrophil count.

Table 1. Baseline patient characteristics according to neutrophil recovery phenotype. *P* values determined by Kruskal-Wallis test for continuous variables and chi-squared test for categorical variables. Values in bold indicates $P < 0.05$. ECOG, Eastern Cooperative Oncology Group; SCT, stem cell transplantation; GCB, Germinal Center B-cell subtype; ABC, Activated B-cell subtype; STLV, sum of target lesion volume; MTV, metabolic tumor volume.

	All patients (*n* = 344)	Quick recovery (*n* = 136)	Intermittent recovery (*n* = 144)	Aplastic (*n* = 64)	*P*
Demographic features					
Age, years (range)	64 (19–83)	64 (30–83)	63 (19–79)	65 (19–80)	0.36
Sex (female)	142 (41%)	38 (28%)	71 (49%)	33 (52%)	**<0.001**
Median ECOG at lymphodepletion (IQR)	1 (0–1)	1 (0–1)	1 (0–1)	1 (1–2)	**<0.001**
International Prognostic Index (IPI, IQR)	3 (2–4), *N* = 322	3 (2–4), *N* = 129	2 (2–3), *N* = 135	3 (2–4), *N* = 58	0.08
Prior therapy					
Median lines of prior therapy (excluding bridging, IQR)	3 (2–4)	3 (2–4)	3 (2–4)	3 (2–4)	0.73
Prior autologous SCT	88 (26%)	31 (23%)	41 (28%)	16 (25%)	0.55
Prior bridging therapy	262 (76%)	97 (71%)	107 (74%)	58 (91%)	**<0.001**
Steroids only	30 (11.5%)	12 (16.5%)	12 (11.2%)	2 (3.5%)	**0.05**
Radiation only	35 (13.3%)	12 (16.5%)	15 (14.0%)	4 (6.9%)	
Immunomodul./Targeted	9 (11.5%)	10 (13.4%)	12 (11.2%)	5 (8.6%)	
Chemotherapy-based	49 (63.7%)	38 (53.6%)	68 (63.6%)	47 (81.0%)	
CAR product					
Tisagenlecleucel	136 (40%)	62 (46%)	46 (32%)	28 (44%)	**0.05**
Axicabtagene ciloleucel	208 (60%)	74 (54%)	98 (68%)	36 (56%)	
Disease features					
Transformed lymphoma (trFL, trMCL, trMALT, trCLL, trHL)	79 (23%)	28 (21%)	38 (26%)	13 (20%)	0.44
BM infiltration	50/315 (16%)	13/128 (10%)	20/132 (15%)	17/55 (31%)	**0.002**
Double/Triple expressor status	137/328 (42%)	53/133 (40%)	49/137 (36%)	33/58 (57%)	**0.02**
Double/Triple-hit status	42/328 (13%)	20/133 (15%)	16/137 (12%)	6/58 (10%)	0.59
Non-GCB/ABC-like	102/328 (31%)	37/133 (28%)	42/137 (31%)	23/58 (40%)	0.26
Tumor burden					
Median LDH, 95% CI (U/liter)	265 (253–288)	254 (238–271)	266 (241–325)	298 (263–390)	**0.04**
STLV (mm^3, IQR)*	87.5 (21.4–265)	41.7 (10.9–123)	40.6 (5.7–255)	444.4 (171–515)	**0.0045**
MTV (mm^3, IQR)†	71.6 (20.9–273)	54.94 (9.71–219)	105.3 (27.93–315.9)	184.3 (35.41–293.0)	0.45
Baseline inflammatory state					
C-reactive protein (mg/dl), 95% CI	1.13 (0.86–1.50)	1.04 (0.74–1.40)	0.87 (0.66–1.46)	2.76 (1.38–4.08)	**0.01**
Ferritin (ng/ml), 95% CI	512 (438–583)	381 (279–512)	493 (370–595)	1110 (812–1850)	**<0.001**
Baseline hematopoietic reserve					
Absolute lymphocyte count (G/liter), 95% CI	620 (570–700) *N* = 324	700 (550–780) *N* = 133	600 (500–700) *N* = 137	580 (450–700) *N* = 54	0.63
Absolute neutrophil count (G/liter), 95% CI	2570 (2360–2870)	3320 (2900–3600)	2380 (2080–2760)	1410 (1080–2020)	**<0.001**
Platelet count (G/liter), 95% CI	157 (146–171)	174 (156–190)	162 (147–180)	107 (79–137)	**<0.001**
Hemoglobin (g/dl), 95% CI	10.3 (10.0–10.5)	10.7 (10.2–11.1)	10.3 (10.0–10.6)	9.1 (8.8–9.7)	**<0.001**
CAR-HEMATOTOX score (median, 95% CI)	2 (1–2)	1 (1–1)	1 (1–2)	3 (3–4)	**<0.001**

*Measurement available in 53 patients (LMU cohort). †Measurement available in 95 patients (Moffitt cohort).

phenotypes (median hospital stay in days, Q versus I versus A: 15 versus 19 versus 21 days, fig. S3). However, no statistically significant difference in hospitalization duration was noted between the intermittent and aplastic phenotypes ($P > 0.9$).

Influence of neutrophil recovery phenotypes on post–CAR-T clinical outcomes

Next, we assessed the relationship between neutrophil recovery phenotypes and clinical outcomes. We observed significant differences in progression-free survival (PFS; $P < 0.0001$, Fig. 2A) and overall survival (OS; $P = 0.0007$, Fig. 2B) by phenotype. Unexpectedly, the intermittent group, characterized by recurrent neutrophil dips (e.g., biphasic neutropenia), exhibited the best survival outcomes (1-year PFS, 51%; 1-year OS, 68%). While the quick phenotype was characterized by an intermediate survival (1-year PFS, 34%; 1-year OS, 59%), both PFS and OS were especially poor in the aplastic patients (1-year PFS, 26%; 1-year OS, 46%). Median PFS was 4 versus 20 versus 3 months (Q versus I versus A, $P < 0.001$, Fig. 2A); median OS was 23 months versus not-reached versus 8 months (Q versus I versus A, $P < 0.001$). Compared to the aplastic phenotype, we observed a significantly reduced hazard ratio for progression in the quick cohort (HR_{PFS} Q versus A: 0.69, 95% CI 0.31 to 0.65) and especially in the intermittent cohort (HR_{PFS} I versus A: 0.45, 95% CI 0.31 to 0.65) (Fig. 2A). Similar hazard ratio differences were noted for OS (Fig. 2B). Furthermore, we noted significantly inferior PFS in the quick compared to the intermittent patients (HR_{PFS} Q versus I: 1.55, 95% CI 1.13 to 2.13), though statistical significance did not extend to OS (HR_{OS} Q versus I: 1.27, 95% CI 0.87 to 1.86).

Next, we studied the phenotypes using a multivariable Cox regression proportional hazards model for PFS and OS, adjusting for other relevant baseline prognostic factors (e.g., CRP, ferritin, LDH, and ECOG) (Fig. 2, C and D). In terms of the other covariates, we confirmed the previously established negative prognostic impact of elevated baseline ferritin and LDH for both PFS and OS (*15*, *25*). Poor performance status was also associated with significantly inferior OS (adjusted HR_{OS} 1.59, 95% CI 1.04 to 2.42), but not PFS. The intermittent phenotype was independently associated with superior PFS (aHR_{PFS} 0.60, 95% CI 0.43 to 0.82, Fig. 2C), with a trend toward improved OS (aHR_{OS} 0.68, 95% CI 0.46 to 1.01, Fig. 2D). On the other hand, the aplastic phenotype did not represent an independent risk factor of PFS and OS. Together, these findings indicate that a phenotype characterized by recurrent neutrophil dips represented an independent positive prognostic marker of CAR-T survival outcomes. In contrast, aplastic neutrophil recovery was associated with adverse treatment outcomes, though not independently of baseline CRP, LDH, and performance status.

The intermittent phenotype is characterized by decreasing inflammation over time, while the aplastic phenotype is associated with high peak IL-6 and ferritin levels

To understand potential determinants of the observed survival discrepancies, we next studied peak inflammatory markers and their changes between lymphodepletion and day 30. Notably, we observed significantly elevated peak IL-6 levels in patients with aplastic as opposed to biphasic or quick recovery (A versus I versus Q, median IL-6: 885 versus 577 versus 253 pg/ml, Fig. 3A). Furthermore, peak serum ferritin levels were significantly increased in the aplastic patients (A versus I versus Q, median IL-6: 1785 versus 973 versus 742 μg/liter, Fig. 3B). On the other hand, no statistically significant difference in peak CRP was noted between phenotype groups (Fig. 3C). When comparing pre– to post–CAR-T therapy changes of serum markers in the intermittent group, we observed a significant reduction of LDH (day 30-to-pre-lymphodepletion fold change: 0.8, 95% CI 0.7 to 0.9, Fig. 3D), ferritin (0.8, 95% CI 0.6 to 1.1, Fig. 3E), and especially CRP levels (0.07, 95% CI 0.05 to 0.1, Fig. 3F). On the other hand, the aplastic patients exhibited a significant increase of serum ferritin at day 30 (1.3, 95% CI 1.1 to 1.9). Fold change differences were particularly evident when comparing the intermittent to the other two phenotypes.

Multivariable binary logistic analysis for the aplastic versus non-aplastic phenotype

When studying the influence of demographic, laboratory, and disease-related factors in a binary logistic regression analysis, we found that the aplastic phenotype was significantly associated with impaired baseline hematopoietic reserve (e.g., low hemoglobin, ANC, and platelet count), increased baseline inflammation (e.g., high CRP and ferritin), and BM infiltration, poor ECOG, double/triple expressor status, increased IPI, and elevated LDH (Table 2). Neither high-grade CRS or ICANS nor CAR product (Tisa-cel versus Axi-cel) was linked to the aplastic phenotype. While peak ferritin increased the risk for the aplastic phenotype, the hazard ratio was diminished compared to baseline ferritin (OR 2.98 versus 4.04). On multivariable regression of baseline risk factors ($n = 344$), the aplastic phenotype was independently associated with the presence of BM infiltration (adjusted OR = 3.2, 95% CI 1.44 to 6.95, $P = 0.004$), ANC (aOR = 0.28, 95% CI 0.12 to 0.63, $P = 0.002$), and ferritin (aOR = 2.3, 95% CI 1.05 to 5.21, $P = 0.039$). Of interest, borderline significance was noted for the association between female sex and the aplastic phenotype (aOR = 3.2, 95% CI 1.4 to 7.0, $P = 0.054$). Together, these findings underline the role of pre–CAR-T cytopenia and inflammation as well as lymphoma BM involvement in driving the aplastic phenotype.

Increased (CAR) T cell expansion and persistence in patients with biphasic neutrophil recovery

The expansion and persistence of CAR T cell populations was assessed by flow cytometry in a subcohort of 104 patients with longitudinal sampling. No difference in peak CAR expansion was noted when comparing patients treated with Axi-cel versus Tisa-cel (fig. S1C). When studying $CD3^+$ CAR T cell dynamics over time, we found that patients with intermittent neutrophil recovery displayed both an earlier and more pronounced expansion peak, and longer CAR-T persistence compared to their quick and aplastic counterparts (Fig. 4A). As a result, the area under the expansion curve (days 0 to 120) was significantly increased in the intermittent cohort. These findings were particularly evident for the $CD3^+CD8^+$ CAR T cell population (Fig. 4B), but also noted for the $CD3^+$ $CD8^-$ CAR T cell population (Fig. 4C). On the other hand, the aplastic and quick cohorts did not exhibit statistically significant differences in CAR-T expansion kinetics. Similar patterns were observed in an analysis of non–CAR-bearing (endogenous) T cell populations in 134 patients with available measurements (fig. S2). As expected, T cell lymphopenia persisted in the patients with aplastic neutrophil recovery (fig. S4, A and B), indicating profound cellular immunosuppression as a potential contributing factor for the high infection rate observed in this patient population (Fig. 1D). While absolute $CD8^+$ T-lymphocyte populations were

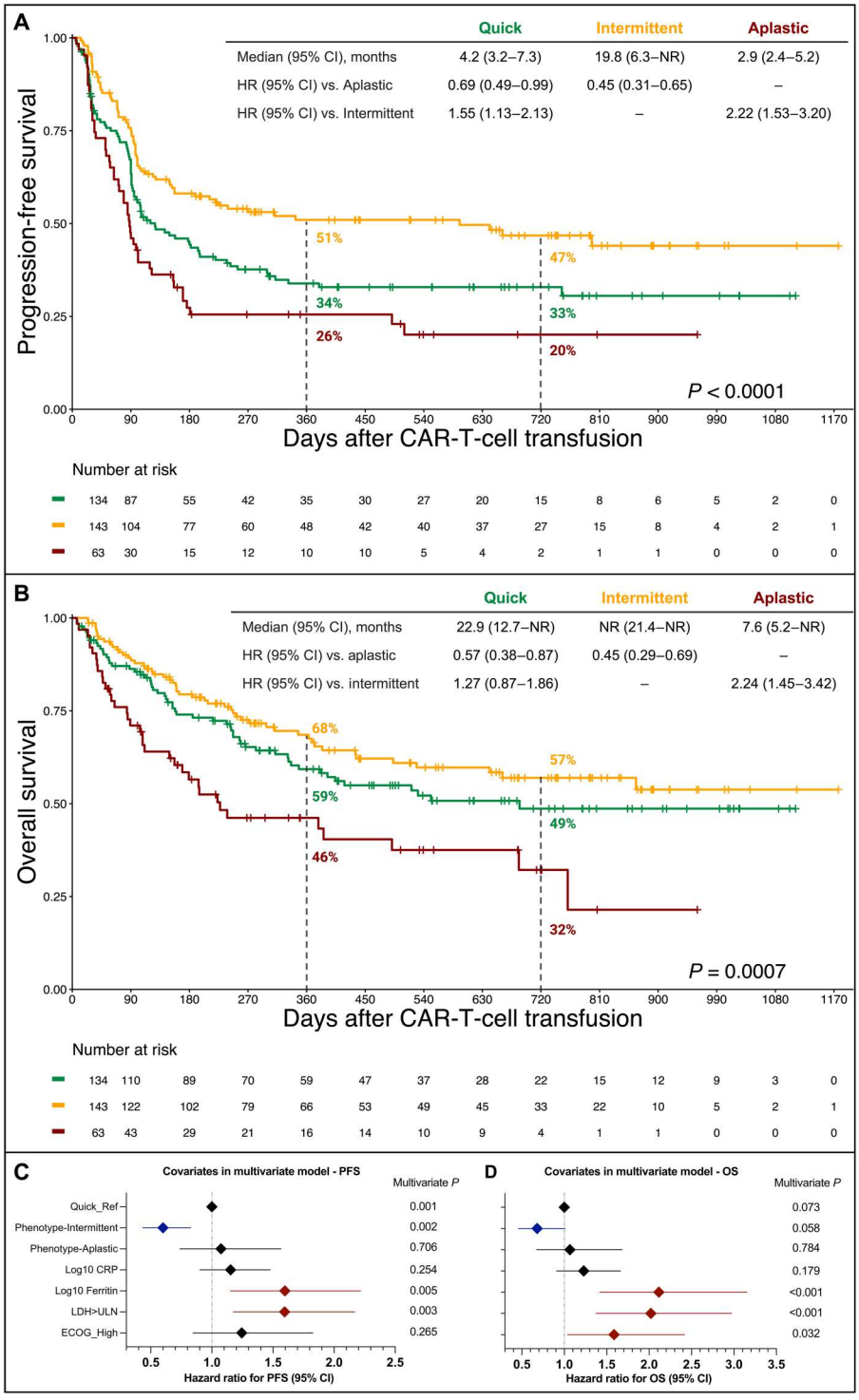

Fig. 2. Influence of neutrophil recovery phenotypes on post–CAR-T clinical outcomes. (**A** and **B**) Kaplan-Meier estimates of PFS (A) and OS (B) by neutrophil recovery phenotype. The median PFS and OS in months for each phenotype group is depicted on the upper right graph inset together with the hazard ratio and 95% CI determined by univariate Cox regression model comparing the respective phenotype groups. The 1-year PFS and OS rate is superimposed above the respective PFS/OS curve for each phenotype group, while the *P* value of the Mantel-Cox log-rank test is shown on the bottom right of the graph. (**C** and **D**) Forest plots of the multivariable analysis performed using Cox proportional hazards modeling for PFS (C) and OS (D). The following covariates were incorporated into the multivariable model: neutrophil recovery phenotype (reference = quick recovery), CRP and ferritin at lymphodepletion (both $\log_{10}$ transformed), LDH greater than the upper limit of normal, ECOG performance status ≥2. Adjusted *P* values accounting for the respective covariates are displayed on the graph inset. Variables reaching statistical significance ($P < 0.05$) are highlighted in red (increased risk) or blue (decreased risk).

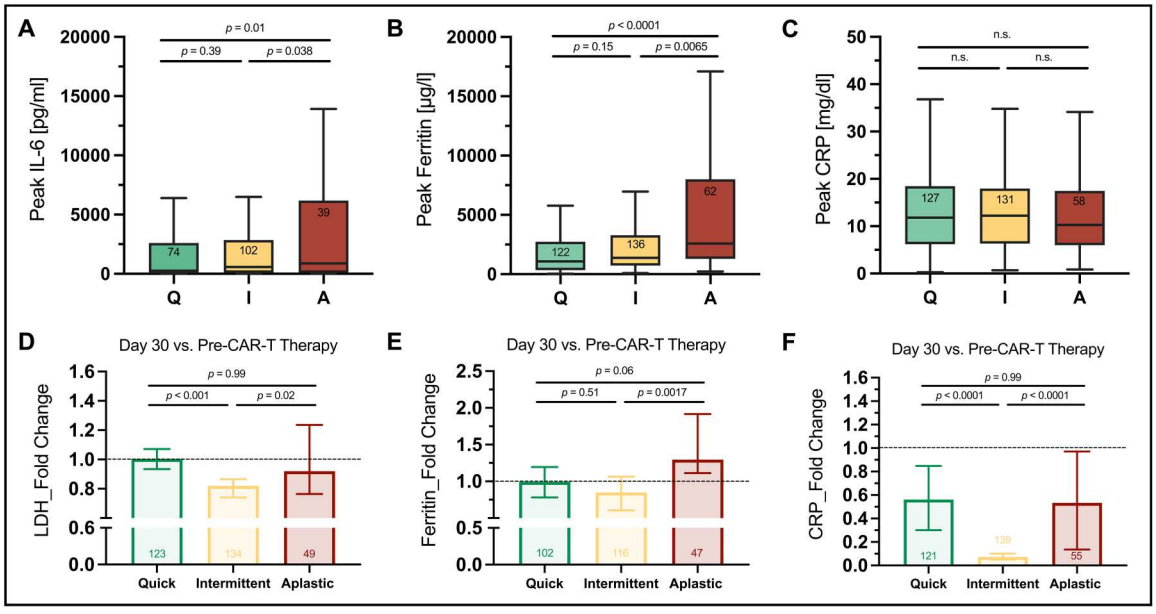

Fig. 3. Dynamic changes of serum markers over time by neutrophil recovery phenotype. (**A** to **C**) Peak serum levels of interleukin-6 (A), ferritin (B), and CRP (C) measured during the first 30 days after CAR-T infusion. (**D** to **F**) Fold change of LDH (D), ferritin (E), and CRP (F) between pre-lymphodepletion measurements and the day 30 measurements. The *P* value of the Kruskal-Wallis test and Dunn's multiple comparison test is depicted.

comparable between the intermittent and quick conditions (fig. S4C), the CD8-to-white blood cell count (WBC) ratio was increased in the intermittent cohort (fig. S4D).

Unfavorable relation of CAR T cell expansion to baseline tumor load and inflammation with the aplastic phenotype

Previous reports have established that the relationship of CAR T cell expansion to baseline tumor burden and inflammatory state is of particular prognostic interest (*25*, *26*). Peak CAR T cell expansion measurements were available in an additional 42 patients (total n = 146) and separated into quartiles to harmonize quantification methods. We noted a trend toward less frequent occurrence of the quick phenotype in high expanders (23% versus 37%, P = 0.1, Fig. 5A). While the quick phenotype constituted the dominant phenotype in patients with the lowest CAR-T expansion (quartile 1 = Q1), the intermittent phenotype was over-represented in the highest CAR-T expanders (Q4) (Fig. 5B). While the aplastic patients were well represented in the high expansion groups (Q3 and Q4), these patients also exhibited high baseline LDH and ferritin, indicative of a higher baseline tumor burden, or "hill to climb" (top right quadrants, Fig. 5, C and D). They also commonly displayed the combination of low expansion and high tumor burden/inflammation, a particularly adverse risk scenario (top left quadrants). Conversely, the quick cohort was characterized by both low CAR-T expansion and low LDH/ferritin (lower left quadrants). Finally, biphasic neutrophil recovery was associated with the advantageous combination of high CAR-T expansion and reduced surrogate markers of tumor burden (lower right quadrants).

Serum proteome analysis revealed progressive immune dysregulation and endothelial dysfunction in the aplastic patients

The serum proteome was explored in samples from 56 lymphoma patients across four time points per patient (days 0, 4, 14, and 28). We encountered a total of 215 samples resulting in 21.436 unique data points. Principal components analysis of the Normalized Protein eXpression (NPX) distribution did not detect outliers and only a single sample was flagged with a quality control warning (fig. S5). While a high degree of overlap was noted between the two- and three-way comparison of neutrophil recovery phenotypes, a higher number of proteins exhibited significant differences when comparing the aplastic versus non-aplastic phenotypes directly (fig. S6). To identify proteins differential between the aplastic (n = 11) and non-aplastic (n = 45) conditions, linear mixed models (LMMs) were fitted to each patient accounting for both phenotype status and time effects and adjusting for age, sex, and patient baseline. The largest number of differences was observed at the last time point (day 28) (Fig. 6A). Still, we found that significant protein-level changes were already present before CAR-T infusion (day 0) in the patients who subsequently went on to develop aplastic neutrophil recovery. This included significant up-regulation of inhibitory soluble T cell checkpoint ligands *Gal-9* (adjusted P = 0.04) and *PD-L2* (adjusted P = 0.0052), while the stimulatory T cell ligand TNFSF14 (LIGHT) was down-regulated (Fig. 6C), consistent with a T cell suppressive cytokine micromilieu. Overall, we found that 20 proteins displayed significant differences between the aplastic and non-aplastic groups in the LMM analysis (Fig. 6B and figs. S7 and S8), with 9 of these proteins demonstrating a significant interaction effect, indicating that differences varied across the measured time points. Hierarchical clustering of patients using the differentially expressed candidate proteins demonstrated a clear separation of the majority of aplastic from non-aplastic patients, particularly on

Table 2. Univariable and multivariable binary logistic regression analysis for aplastic versus non-aplastic phenotype. Only covariates with a *P* value <0.1 on univariate analysis were introduced into the multivariable model and these rows are highlighted in bold. The exception was peak ferritin, which was omitted based on the results of the univariate analysis for baseline ferritin so as to avoid collinearity. Abbreviations: ABC, activated B cell type; GCB, germinal center B cell like; ECOG, Eastern Cooperative Oncology Group; BM, bone marrow.

Covariate	*N*	Univariate analysis			Multivariable analysis		
		Odds ratio	95% CI	*P* value	Adjusted OR	95% CI	*P* value
Pre–CAR-T (sorted by P value)							
Prior ASCT	344	0.96	0.52–1.80	0.91	-	-	-
Age	316	0.998	0.975–1.023	0.90	-	-	-
Absolute lymphocyte count (log10)	324	0.89	0.44–1.83	0.76	-	-	-
Lines of prior therapy (excl. bridging)	344	1.04	0.88–1.24	0.64	-	-	-
Disease entity (transformed lymphoma)	344	0.83	0.42–1.61	0.58	-	-	-
Double/Triple hit status	328	0.75	0.30–1.87	0.54	-	-	-
Cell of origin (ABC/non-GCB type)	328	1.59	0.88–2.86	0.12	-	-	-
Gender (female)	**344**	**1.67**	**0.97–2.88**	**0.07**	**1.98**	**0.98–3.96**	**0.054**
Lactate dehydrogenase (LDH) > ULN	**344**	**1.83**	**1.03–3.24**	**0.04**	1.01	0.46–2.21	0.98
International Prognostic Index (IPI ≥ 3)	**322**	**1.87**	**1.04–3.39**	**0.04**	1.46	0.68–3.16	0.33
Double/Triple expressor status	**328**	**2.17**	**1.22–3.86**	**0.008**	1.64	0.84–3.22	0.15
C-reactive protein (CRP, log10)	**344**	**1.81**	**1.20–2.75**	**0.005**	0.89	0.47–1.68	0.71
ECOG performance status ≥ 2	**344**	**2.68**	**1.36–5.27**	**0.004**	1.25	0.49–3.16	0.64
BM infiltration (present)	**315**	**3.08**	**1.56–6.07**	**0.001**	**3.16**	**1.44–6.95**	**0.004**
Hemoglobin	**344**	**0.67**	**0.56–0.79**	**<0.001**	0.84	0.64–1.11	0.22
Absolute neutrophil count (log10)	**344**	**0.25**	**0.13–0.47**	**<0.001**	**0.28**	**0.12–0.63**	**0.002**
Platelet count (log10)	**344**	**0.15**	**0.07–0.35**	**<0.001**	0.63	0.19–2.05	0.44
Ferritin (log10)	**344**	**4.04**	**2.29–7.12**	**<0.001**	**2.33**	**1.05–5.21**	**0.039**
Post–CAR-T (sorted by P value)							
Steroid use	343	1.08	0.62–1.88	0.78	-	-	-
Peak CRP (log10)	344	1.12	0.59–2.10	0.73	-	-	-
CAR T cell product (Tisa-cel)	344	1.24	0.72–2.15	0.45	-	-	-
CRS grade (ASTCT grade ≥ 3)	343	1.55	0.66–3.64	0.31	-	-	-
Peak IL-6 (log10)	215	1.20	0.85–1.70	0.29	-	-	-
ICANS grade (ASTCT grade ≥ 3)	343	1.67	0.84–3.29	0.14	-	-	-
Tocilizumab use	343	1.53	0.87–2.69	0.14	-	-	-
Peak ferritin (log10)	**317**	**2.98**	**1.78–5.01**	**<0.001**	*	*	*

day 0 and day 28 (fig. S9). Notably, we observed progressive down-regulation of the endothelial and angiogenetic markers *ANGPT1* (adjusted $P = 0.0024$), *EGF* (adjusted $P = 0.01$), and *PDGFB* (adjusted $P = 0.0061$) over time in the patients with aplastic neutrophil recovery (Fig. 6D). This was accompanied by immune dysregulation as indicated by the marked down-regulation of *CD40L* (adjusted $P = 0.02$, Fig. 6E) and up-regulation of *MCP-1* (adjusted $P = 0.0085$, Fig. 6E). Furthermore, we noted significant up-regulation of *IL-15* (adjusted $P = 0.04$) and *IL-18* (adjusted $P = 0.01$) in the aplastic patients, both of which play an important role in the production of *IFN*-γ from macrophages, NK cells, and T cells (*27*, *28*). A trend toward increased serum *IFN*-γ was noted in the aplastic patients starting on day 14 (fig. S10). We confirmed higher peak serum *IFN*-γ levels in the aplastic group, along with increased *IL-15* and *TNF*-α levels, in a second independent cohort using a previously established automated immunoassay (Fig. 6F) (*29*). This assay further confirmed significant down-regulation of *ANGPT1*, resulting in an increased Angiopoietin-2 to Angiopoietin-1 (Ang-2/1) ratio. Together, these longitudinal proteomic analyses provide a biological correlate for progressive endothelial and platelet dysfunction, immune dysregulation, and macrophage activation in patients with aplastic neutrophil recovery.

DISCUSSION

In this multicenter observational study of 344 R/R LBCL patients, we report differential disease outcomes depending on the observed pattern of cytopenia after CD19 CAR-T therapy. Compared to quick neutrophil recovery, we demonstrate that biphasic recovery (intermittent phenotype) is associated with excellent PFS/OS,

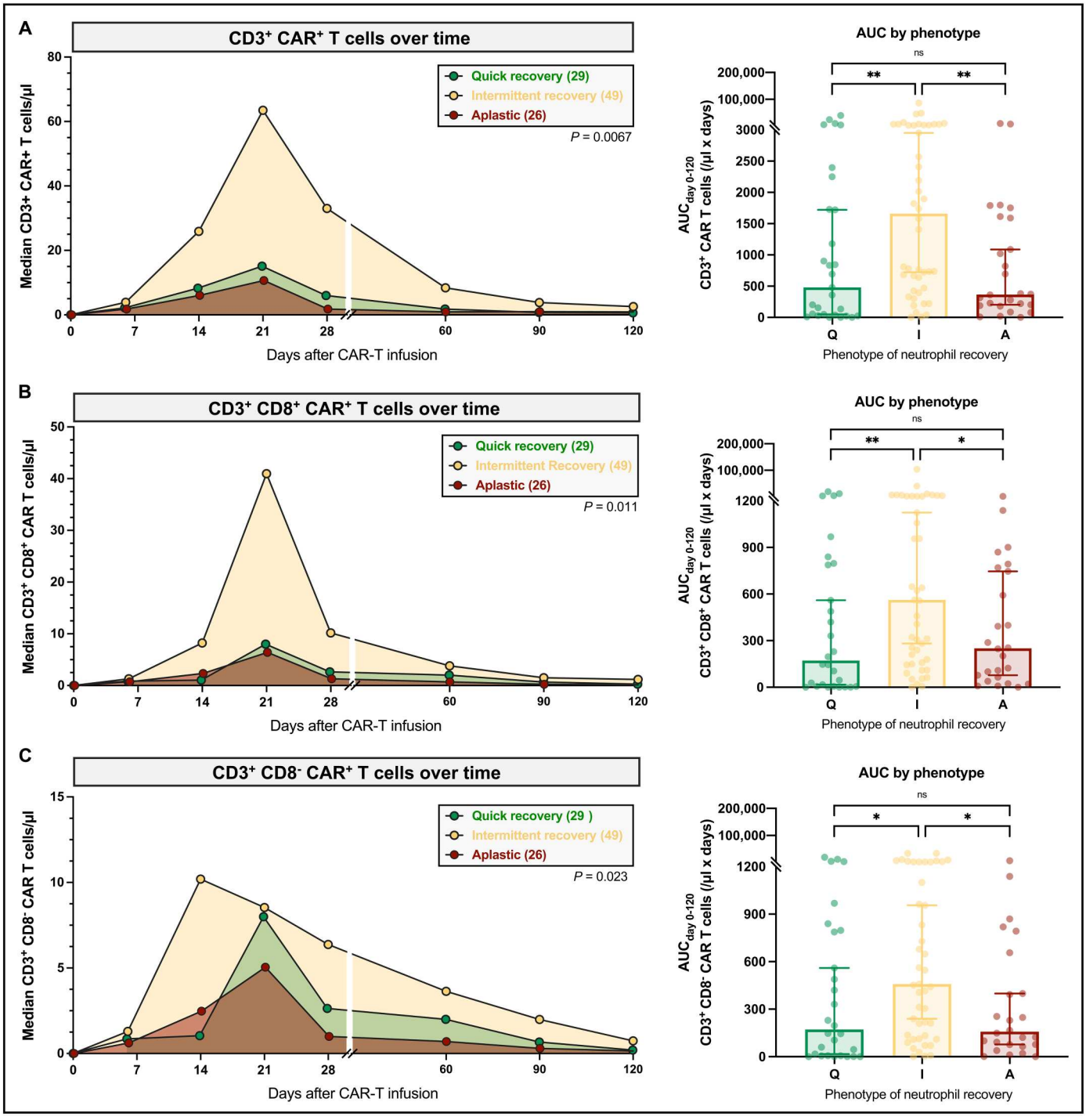

Fig. 4. CAR T cell expansion over time by neutrophil recovery phenotype. CAR T cell expansion kinetics over time as determined by longitudinal immunomonitoring using flow cytometry (days 0, 4 to 7, 14, 21, 28, 60, 90, and 120) in 104 patients treated across three CAR-T centers (Barcelona, LMU, Erlangen). (**A** to **C**) Median absolute number of $CD3^+$ (A), $CD3^+/CD8^+$ (B), and $CD3^+/CD8^-$ (C) CAR T cells over time by neutrophil recovery phenotype (left); area under the expansion curve (right). The total area under the expansion curve was compared across phenotype groups using the Kruskal-Wallis test with correction for multiple testing by controlling the false discovery rate (two-stage step-up method of Benjamini, Krieger, and Yekutieli). Significance values: $^*P < 0.05$ and $^{**}P < 0.01$; ns, not significant.

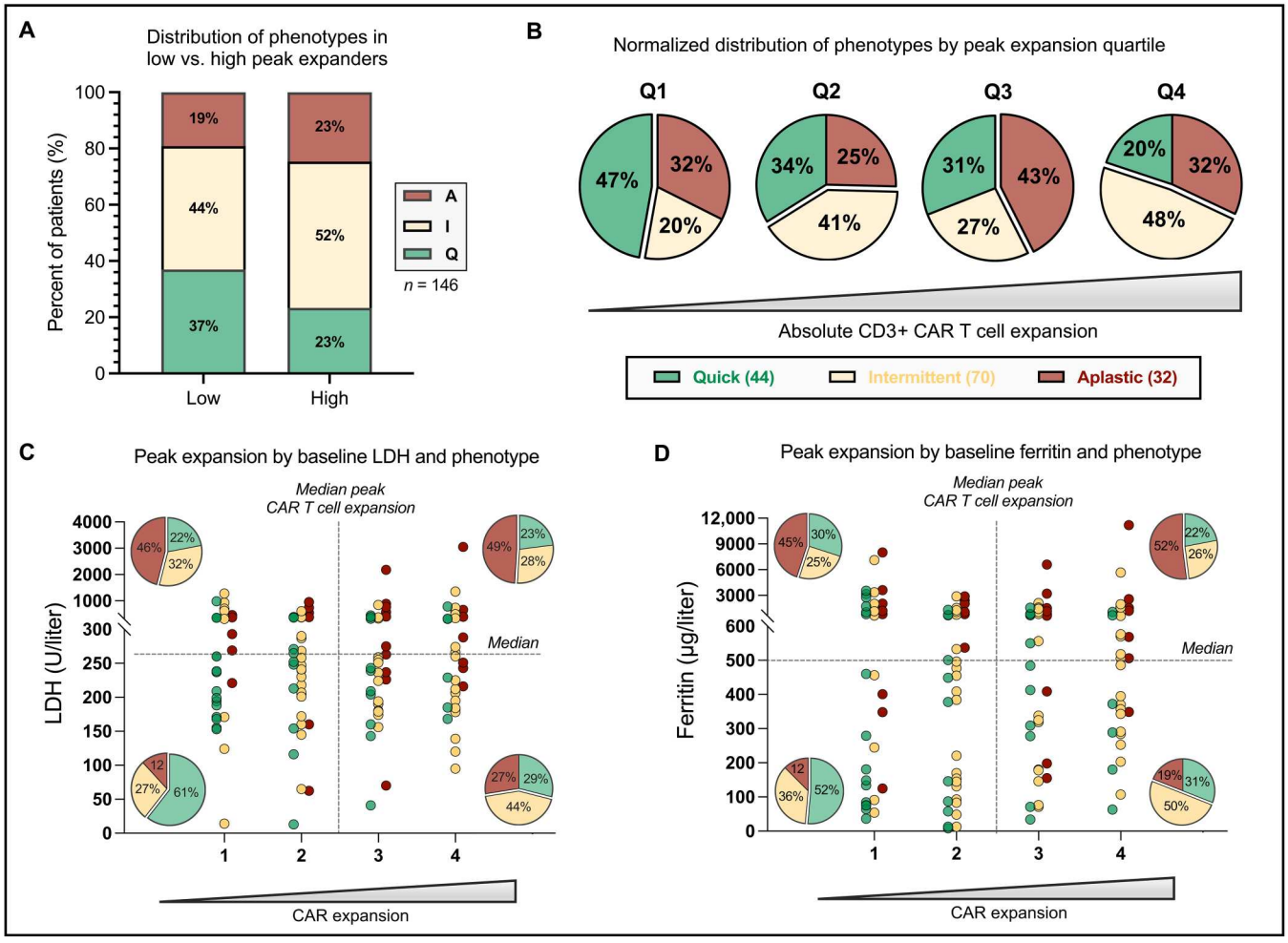

Fig. 5. Relationship between post–CAR-T hematopoietic recovery, CAR T cell expansion, and baseline tumor burden and inflammation. Peak CAR expansion was stratified into four quartiles in 146 patients to account for differences in CAR quantification across centers (42 additional patients with available peak CAR expansion data compared to Fig. 4). (**A**) Distribution of neutrophil recovery phenotypes comparing high CAR expanders (above median) versus low expanders (below median). (**B**) Normalized distribution of neutrophil recovery phenotypes within each quartile CAR-T expansion (absolute CD3+ CAR T cell expansion increasing from left to right). (**C** and **D**) Scatterplot depicting baseline LDH (C) and ferritin (D) on the *y* axis and the quartiles of peak CAR-T expansion on the *x* axis. The normalized distribution of phenotypes is superimposed into the graph for each quadrant.

robust CAR T cell expansion, and decreasing systemic inflammation over time. Conversely, sustained neutropenia (aplastic phenotype) resulted in increased rates of severe infections and NRM, poor PFS/OS, and suboptimal CAR T cell expansion in relation to baseline tumor load. Pathophysiologically, the aplastic group exhibited high serum levels of T cell inhibitory ligands such as *PD-L2* and *Gal-9*, along with markers of macrophage activation, cytokine inflammation, and endothelial dysfunction.

The reported incidence of hematological toxicity (e.g., distribution of phenotypes and neutropenia duration), as well as the underlying patient characteristics and clinical outcomes were consistent with prior publications (*10*, *13*, *16*, *30*). While similar rates of aplastic neutrophil recovery were observed by CAR product, Axi-cel patients more commonly exhibited the intermittent phenotype, in line with other retrospective real-world studies demonstrating delayed hematopoietic reconstitution with Axi-cel compared to Tisa-cel (*31*, *32*). In contrast to previous reports (*24*, *32*), we did not identify a significant correlation between high-grade CRS or ICANS and the aplastic phenotype on both uni- and multivariable analysis (Table 2). Rather, the inflammatory state and hematopoietic function at baseline were the predominant risk factors driving profound cytotoxicity after CAR-T therapy. Such high levels of systemic inflammatory markers may reflect not only an inflamed lymphoma microenvironment (*25*) but also inflammation within the hematopoietic niche. Patients with impaired hematopoietic function (as reflected by trilineage cytopenia) may be at particular risk for inflammation-mediated myelosuppression. The fact that the aplastic group more frequently received chemotherapy-based bridging therapy underlines that cytotoxic treatment immediately prior to CAR-T therapy can predispose for prolonged cytopenias after CAR T cell infusion, especially in patients with poor marrow reserve and high-risk lymphoma (*33*) (see "note added in proof"). Of note, BM infiltration represented an independent adverse risk factor for hematotoxicity in our cohort. The presence of lymphoma within the hematopoietic niche likely predisposes for local inflammatory stress due to the interaction of (CAR) T cells, bystander cells,

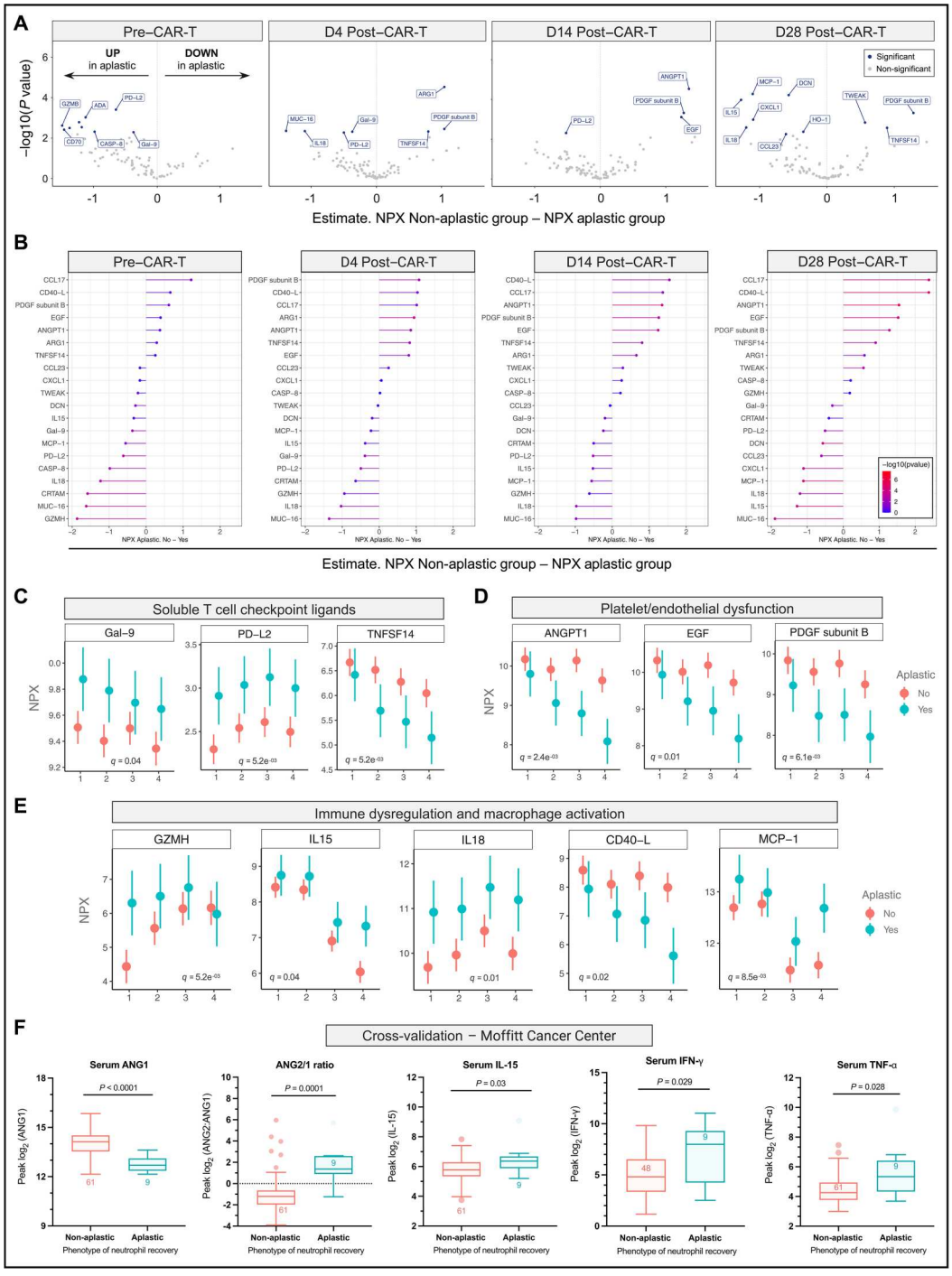

Fig. 6. The aplastic phenotype displays a serum proteome signature consistent with progressive endothelial dysfunction and immune dysregulation. (**A**) Volcano plots showing the estimated mean difference between the non-aplastic and aplastic patient groups (*x* axis), and corresponding $-\log_{10}$ (*P* values) (*y* axis). Blue colors indicate proteins that passed the multiple testing adjusted *P* value threshold of $P < 0.05$. Each panel corresponds to one time point (days 0, 4, 14, and 28). (**B**) Differential expression per time point (from left to right) of the 20 proteins that differed between the non-aplastic and aplastic groups (significant main and/or interaction effect). The *x* axis shows the estimated mean NPX difference between non-aplastic and aplastic patients, with colors indicating the corresponding *P* values (not corrected for multiple testing). Each panel corresponds to one time point, with proteins sorted by their NPX level changes (right: down-regulated; left: up-regulated in the aplastic group). As NPX is expressed on a log2 scale, an increase of 1 NPX corresponds to a doubling of the serum protein concentration. (**C** to **E**) Point range plots of top candidate proteins of interest related to soluble T cell checkpoint ligands (C), platelet and endothelial function (D), and immune response and macrophage activation (E). The graph represents the linear mixed model (LMM) estimates of mean NPX levels (*y* axis) per time point (*x* axis). The *P* value corrected for multiple testing (*q* value) is superimposed on each panel. (**F**) Validation of peak serum levels of key candidate markers in a cohort of 70 patients from the Moffitt Cancer Center. From left to right: angiopoietin-1, angiopoietin 2–to–angiopoietin 1 ratio, interleukin-15, interferon-γ, and tumor necrosis factor–α (TNF-α). Logarithm transformation was utilized to allow visualization of data points on the graphs.

proinflammatory cytokines, and the hematopoietic stem and progenitor cell compartment.

Notably, we found that the soluble immune checkpoint molecules *PD-L2* and *Gal-9* were already up-regulated at baseline in the patients who subsequently developed the aplastic phenotype, hinting at potential interactions between the underlying lymphoma and the endogenous T cell repertoire (*34*–*38*). For example, *Galectin-9* serves as the natural ligand of the immune receptor TIM3 (*35*). The protein can modulate intratumoral TIM-3$^+$ cytotoxic CD8$^+$ T cells and immunosuppressive regulatory T cells, with high expression levels being linked to a poor prognosis across multiple human cancers (*39*). This type of immune dysregulation that is both inflammatory and T cell suppressive provides an explanation for the paradoxical finding that patients with the aplastic phenotype had lower CAR T cell expansion (and inferior treatment outcomes) than those with the intermittent phenotype. Aplastic patients exhibit a particularly high risk of infection (44% with severe infections), which may be due to prolonged neutropenia occurring in combination with

functional T cell suppression and the prolonged T cell deficits reported in CAR-T patients (*40*, *41*). Furthermore, we observed up-regulation of *Granzyme B*, a hallmark of immune activation in cytotoxic lymphocytes in hemophagocytic lymphohistiocytosis (*35*). Notably, this coincided with high baseline levels of serum ferritin, which then subsequently increased over time (median fold change at day 30 = 1.3, 95% CI 1.1 to 1.9). This could also suggest a certain degree of overlap with sHLH/MAS, a well-described side effect of CAR-T therapy (especially with CD22-directed CAR products) (*42*, *43*), which is clinically characterized by pancytopenia and also features similar elevations of *IFN-γ, MCP-1, IL-15,* and *IL-18* (*44*–*48*). Other studies have delineated a central role for *IL-15* in enhancing CAR-T–mediated antitumor activity by promoting a stem cell memory T cell phenotype (*49*, *50*), suggesting a fine balance between treatment efficacy and excessive immunotoxicity. The increase of serum interferon-γ (IFN-γ) levels in the aplastic patients was more pronounced with the more focused Ella Automated Immunoassay System compared to the multiplexed Olink platform, highlighting assay-dependent differences in biomarker detection. Overall, the role of IFN-γ in the context of CAR-T–related hematotoxicity is of particular interest, as this proinflammatory cytokine represents a mediator of hematopoiesis and has been demonstrated to reduce stem cell cycling (*51*, *52*). While acute IFN-γ is a key potentiator of T cell function, we and others have previously found that chronic interferon signaling is associated with poor response to immunotherapies, and is associated with the up-regulation of multiple T cell suppressive checkpoint ligands leading to T cell dysfunction (*25*, *53*–*55*). Further investigations are needed to understand the relationship between tumor interferon signaling, the effects of chronic IFN-γ in the peripheral blood, and hematotoxicity. Of interest, we detected only minimal differences between the intermittent and quick groups in the serum proteomic analysis. On the one hand, the patient numbers for the Olink analysis may have been too small to identify features that are unique to the intermittent phenotype. On the other hand, the differences between the intermittent and quick patients may primarily relate to discrepancies in CAR T cell expansion kinetics.

Recent reports have linked prolonged post-infusion cytopenias to diminished CAR-T efficacy (*56*, *57*). However, our study indicates that qualitative differences in cytopenia (e.g., biphasic versus monophasic) likely provide critical context for any observed survival differences. For example, two patients presenting with an ANC of 500/μl at day 30 may exhibit divergent treatment outcomes, depending on whether they displayed prior count recovery (intermittent) or continuously low peripheral blood counts (aplastic). Notably, patients with biphasic neutrophil recovery exhibited high CAR T cell expansion and persistence (Fig. 4), perhaps reflecting intermittent extravasation of immune cells including CAR T cells into the periphery, BM, and to the lymphomatous tissue (*58*). Similar to hematologic complications of immune checkpoint inhibitors, recurrent neutrophil drops may thus be facilitated by autoreactive (CAR) T cells and persistent inflammatory signals (*18*, *59*). This would be consistent with a natural model of CAR-T–related inflammation proposed by Wei *et al.* (*60*), wherein peripheral CAR T cells redistribute into the BM and other organs after approximately 10 to 21 days, prompting a second decrease in peripheral blood counts and, ideally, ongoing tumor regression. Considering the independent prognostic value of biphasic neutrophil recovery, future studies may prospectively evaluate the utility of this marker as a component of dynamic risk assessment in patients receiving CAR-T therapies. On the other hand, the negative prognostic impact of the aplastic phenotype was attenuated when accounting for other recognized risk factors of CAR-T therapy, indicating that these patients observe coincident poor risk features that likely drive any association with poor clinical outcomes. These data underline that confounding factors need to be considered when interpreting the impact of hematotoxicity on post–CAR-T survival outcomes. Furthermore, the baseline proteomic findings provide mechanistic context for the prognostic value of the CAR-HEMATOTOX score both in regard to the prediction of the aplastic phenotype and clinical outcomes across disease entities (e.g., LBCL, mantle cell lymphoma, and multiple myeloma) (*13*, *33*, *61*) (see "note added in proof"). The Olink results suggest that increased levels of serum inflammatory markers such as CRP or ferritin (incorporated in the CAR-HEMATOTOX score) are associated with a T cell suppressive cytokine micromilieu, and may more fundamentally reflect poor disease biology and an immunohostile tumor microenvironment (*25*, *62*, *63*). Several of the identified Olink markers may be useful to improve upon outcome prediction and could be integrated into dynamic risk models that identify high-risk patients who could benefit from immunomodulatory or other experimental agents.

This study has several relevant limitations. It was retrospective in nature and limited to R/R LBCL patients. While the inclusion of multiple sites represents a strength of the analysis, this comes at the price of heterogeneity in regard to the management of CAR-T–related toxicities including cytopenias. Data on longitudinal in vivo CAR T cell dynamics (Fig. 4) were available in fewer patients than peak CAR expansion measurements (Fig. 5), which may explain the variance in the distribution of phenotypes between both analyses. While we attempted to harmonize CAR-T quantification methods by assigning center-specific quartiles, we cannot exclude that this may have represented a confounding factor for the CAR T cell expansion analysis by phenotype. Other potential driving mechanisms of resistance such as tumor microenvironmental features (*25*) and genomic drivers (*62*, *64*), or product immunogenicity (*65*), could not be considered in this study. Still, these findings are hypothesis-generating and carry several pertinent clinical applications. First and foremost, our data suggest that the underlying mechanisms of intermittent and aplastic neutrophil recovery substantially differ. As a result, one-size-fits-all management approaches to cytopenia are unlikely to meet the needs of all patients equally. While patients with intermittent recovery can be effectively managed with growth factor support, the aplastic group may require escalated measures that facilitate a functional "reset" of the hematopoietic compartment such as a stem cell boost (if available) (*20*). Second, biphasic neutrophil recovery may represent a novel dynamic biomarker of treatment response that warrants further validation in larger patient datasets and for other disease entities in which CAR-T therapies are currently being explored such as multiple myeloma and mantle cell lymphoma. Finally, future studies that examine how the modulation of host hematopoiesis impacts (and potentially enhances) the systemic antitumor efficacy of CAR T cells appear warranted.

In conclusion, these data provide evidence that hematopoietic reconstitution patterns reflect differences in CAR-T expansion kinetics and inflammatory profiles after CD19 CAR-T therapy. Our findings highlight critical interactions between host hematopoiesis and CAR-T efficacy, and suggest that management strategies will

need to be tailored to the underlying pathophysiology of hematotoxicity.

MATERIALS AND METHODS

Patients and data collection

In this multicenter retrospective observational study, we studied toxicity and survival outcomes in 344 patients receiving standard-of-care Axi-cel (n = 208) or Tisa-cel (n = 136) for R/R LBCL after at least two prior treatment lines of therapy. Patients were treated between May 2018 and December 2021 across six international CAR-T centers [Ludwig Maximilian University (LMU) Munich, Tübingen, Erlangen, Berlin Charité, Vall D′Hebron Barcelona, Moffitt Cancer Center]. The patient cohort represents an extension of our previous report (*13*) and includes clinical metadata from an additional 94 patients treated with CD19 CAR-T across the participating sites. Lymphodepleting chemotherapy with fludarabine and cyclophosphamide was administered according to the manufacturer′s instructions (*3*, *4*). Clinical metadata were extracted from medical records and databases with institutional review board approval (LMU Munich: Project No. 19-817; Moffitt Cancer Center: Advarra Pro00024557) (*66*).

Defining hematological toxicity and neutrophil recovery phenotypes

The duration of severe neutropenia was assessed as the total cumulative days with a measured ANC <500/μl between days 0 and + 60 (*10*). All patients were assigned a phenotype of neutrophil recovery according to the following definitions:

1) Quick: sustained neutrophil recovery without a second dip below an ANC <1000/μl.

2) Intermittent: neutrophil recovery (ANC > 1500/μl) followed by a second dip with an ANC <1000/μl after day 21.

3) Aplastic: continuous severe neutropenia (ANC < 500/μl) ≥14 days.

Toxicity grading

CRS and ICANS were graded according to American Society for Transplantation and Cellular Therapy consensus criteria (*67*). Toxicity management and antimicrobial prophylaxis followed institutional guidelines (*13*, *68*). Infection episodes were characterized between the day of CAR-T infusion until day +90 as described previously, with severity being classified on a five-grade scale as mild, moderate, severe, life-threatening, or fatal (*11*, *13*, *69*). Infection episodes were defined as bacterial, viral, or fungal based on microbiologic or histopathologic data or as a clinical syndrome of infection (e.g., pneumonia, cellulitis, and cystitis) based on retrospective chart review.

Clinical outcomes

Efficacy outcomes were assessed according to Lugano criteria (*70*). Kaplan-Meier estimates for PFS and OS were calculated from time of CAR-T infusion, with phenotype groups being compared by log-rank test. Nonrelapse mortality was defined as death after cellular therapy without prior relapse or progression. Duration of hospitalization was determined from start of lymphodepletion until first discharge from hospital.

Multivariable analyses for the aplastic phenotype and survival outcomes

Multivariable analysis of patient-, disease-, and therapy-related factors was performed as binary logistic regression for the aplastic versus non-aplastic phenotypes including variables with a $P < 0.1$ on univariate analysis. The prognostic influence of the neutrophil recovery phenotypes was explored in a multivariable Cox regression proportional hazards model for PFS and OS, adjusting for the baseline prognostic markers CRP, ferritin (both $\log_{10}$ transformed), LDH, and ECOG (*15*, *25*).

(CAR) T cell kinetics

Quantification of CAR T cells was performed by quantitative polymerase chain reaction (n = 42) or by flow cytometry (n = 104) according to institutional protocols as previously described (*25*, *71*). To harmonize CAR T cell expansion across centers, patients were divided into quartiles by their respective peak expansion.

Serum proteomic analysis

The serum proteome was longitudinally characterized across four sequential time points (days 0, 4, 14, and 28) in 56 patients using a 92-protein multiplex proximity extension assay from the Olink platform ("Immuno Oncology Panel," Olink Bioscience). The experimental setup has been described previously (*72*–*74*). Briefly, oligonucleotide-labeled monoclonal or polyclonal antibodies (PEA probes) were utilized to bind target proteins in a pairwise manner and to prevent cross-reactive events. Upon binding, the oligonucleotides come in close proximity and hybridize. After extension, a unique sequence is generated to digitally identify the specific protein assay. To test protein-level differences proteins by patient group (aplastic versus non-aplastic) and time point, we applied an LMM per protein. To account for potential confounding, age and sex were included as fixed effects, while a random effect per patient was included to account for potentially differing baselines. Regression models were fitted using the R-packages lme4 and lmerTest, while plots were generated using the OlinkAnalyze and ggplot2 packages. Protein levels were represented in NPX units, derived from Ct values, and expressed in $\log_2$ scale (e.g., 1 NPX difference = doubling of protein concentration). Key candidate serum markers were validated in 70 patients from the Moffitt Cancer Center using the Ella Automated Immunoassay System (ProteinSimple), which included GM-CSF, interleukins, IFN-γ, TNF-α, and angiopoietin 1 and 2.

Statistical considerations

Kruskal-Wallis test with Dunn′s multiple comparison test was used to explore continuous variables, while Fisher′s exact test and chi-squared test were used to study categorical variables. The d′Agostino Pearson test was used to determine normal distribution. Statistical analysis and data visualization were performed using GraphPad Prism (v9.0), SPSS (IBM, v26.0), and R Statistical Software (v4.1.2).

Note added in proof: Shortly after the acceptance of this manuscript for publication, (*33*) was published in full as "K. Rejeski *et al.*, The CAR-HEMATOTOX score identifies patients at high risk for hematological toxicity, infectious complications, and poor treatment outcomes following brexucabtagene autoleucel for relapsed or refractory MCL. *Am. J. Hematol.* (2023)" and (*61*) was published

in full as "K. Rejeski *et al*., The CAR-HEMATOTOX score as a prognostic model of toxicity and response in patients receiving BCMA-directed CAR-T for relapsed/refractory multiple myeloma. *J. Hematol. Oncol.* **16**, 88 (2023)." Additionally, the following reference was published after this manuscript was accepted for publication, where the term "Immune Effector Cell-Associated Hematotoxicity (ICAHT)" was introduced: "K. Rejeski *et al*., Immune Effector Cell-Associated Hematotoxicity (ICAHT): EHA/EBMT consensus grading and best practice recommendations. *Blood* (2023)."

Supplementary Materials

This PDF file includes:

Tables S1 to S3
Figs. S1 to S10

REFERENCES AND NOTES

1. F. L. Locke, D. B. Miklos, C. A. Jacobson, M. A. Perales, M. J. Kersten, O. O. Oluwole, A. Ghobadi, A. P. Rapoport, J. McGuirk, J. M. Pagel, J. Muñoz, U. Farooq, T. van Meerten, P. M. Reagan, A. Sureda, I. W. Flinn, P. Vandenberghe, K. W. Song, M. Dickinson, M. C. Minnema, P. A. Riedell, L. A. Leslie, S. Chaganti, Y. Yang, S. Filosto, J. Shah, M. Schupp, C. To, P. Cheng, L. I. Gordon, J. R. Westin, Axicabtagene ciloleucel as second-line therapy for large B-cell lymphoma. *N. Engl. J. Med.* **386**, 640–654 (2022).
2. B. D. Shah, A. Ghobadi, O. O. Oluwole, A. C. Logan, N. Boissel, R. D. Cassaday, T. Leguay, M. R. Bishop, M. S. Topp, D. Tzachanis, K. M. O'Dwyer, M. L. Arellano, Y. Lin, M. R. Baer, G. J. Schiller, J. H. Park, M. Subklewe, M. Abedi, M. C. Minnema, W. G. Wierda, D. J. DeAngelo, P. Stiff, D. Jeyakumar, C. Feng, J. Dong, T. Shen, F. Milletti, J. M. Rossi, R. Vezan, B. K. Masouleh, R. Houot, KTE-X19 for relapsed or refractory adult B-cell acute lymphoblastic leukaemia: Phase 2 results of the single-arm, open-label, multicentre ZUMA-3 study. *Lancet* **398**, 491–502 (2021).
3. F. L. Locke, A. Ghobadi, C. A. Jacobson, D. B. Miklos, L. J. Lekakis, O. O. Oluwole, Y. Lin, I. Braunschweig, B. T. Hill, J. M. Timmerman, A. Deol, P. M. Reagan, P. Stiff, I. W. Flinn, U. Farooq, A. Goy, P. A. McSweeney, J. Munoz, T. Siddiqi, J. C. Chavez, A. F. Herrera, N. L. Bartlett, J. S. Wiezorek, L. Navale, A. Xue, Y. Jiang, A. Bot, J. M. Rossi, J. J. Kim, W. Y. Go, S. S. Neelapu, Long-term safety and activity of axicabtagene ciloleucel in refractory large B-cell lymphoma (ZUMA-1): A single-arm, multicentre, phase 1-2 trial. *Lancet Oncol.* **20**, 31–42 (2019).
4. S. J. Schuster, M. R. Bishop, C. S. Tam, E. K. Waller, P. Borchmann, J. P. McGuirk, U. Jäger, S. Jaglowski, C. Andreadis, J. R. Westin, I. Fleury, V. Bachanova, S. R. Foley, P. J. Ho, S. Mielke, J. M. Magenau, H. Holte, S. Pantano, L. B. Pacaud, R. Awasthi, J. Chu, Ö. Anak, G. Salles, R. T. Maziarz, Tisagenlecleucel in adult relapsed or refractory diffuse large B-cell lymphoma. *N. Engl. J. Med.* **380**, 45–56 (2019).
5. M. Wang, J. Munoz, A. Goy, F. L. Locke, C. A. Jacobson, B. T. Hill, J. M. Timmerman, H. Holmes, S. Jaglowski, I. W. Flinn, P. A. McSweeney, D. B. Miklos, J. M. Pagel, M. J. Kersten, N. Milpied, H. Fung, M. S. Topp, R. Houot, A. Beitinjaneh, W. Peng, L. Zheng, J. M. Rossi, R. K. Jain, A. V. Rao, P. M. Reagan, KTE-X19 CAR T-cell therapy in relapsed or refractory mantle-cell lymphoma. *N. Engl. J. Med.* **382**, 1331–1342 (2020).
6. G. Iacoboni, K. Rejeski, G. Villacampa, J. A. van Doesum, A. Chiappella, F. Bonifazi, L. Lopez-Corral, M. van Aalderen, M. Kwon, N. Martínez-Cibrian, S. Bramanti, J. L. Reguera-Ortega, L. Camacho-Arteaga, C. Schmidt, A. Marín-Niebla, M. J. Kersten, A. Martin Garcia-Sancho, P. L. Zinzani, P. Corradini, T. van Meerten, M. Subklewe, P. Barba, Real-world evidence of brexucabtagene autoleucel for the treatment of relapsed or refractory mantle cell lymphoma. *Blood Adv.* **6**, 3606–3610 (2022).
7. A. Shimabukuro-Vornhagen, P. Gödel, M. Subklewe, H. J. Stemmler, H. A. Schlößer, M. Schlaak, M. Kochanek, B. Böll, M. S. von Bergwelt-Baildon, Cytokine release syndrome. *Cancer* **6**, 56 (2018).
8. P. Karschnia, J. T. Jordan, D. A. Forst, I. C. Arrillaga-Romany, T. T. Batchelor, J. M. Baehring, N. F. Clement, L. N. Gonzalez Castro, A. Herlopian, M. V. Maus, M. H. Schwaiblmair, J. D. Soumerai, R. W. Takvorian, E. P. Hochberg, J. A. Barnes, J. S. Abramson, M. J. Frigault, J. Dietrich, Clinical presentation, management, and biomarkers of neurotoxicity after adoptive immunotherapy with CAR T cells. *Blood* **133**, 2212–2221 (2019).
9. K. Wudhikarn, M. Pennisi, M. Garcia-Recio, J. R. Flynn, A. Afuye, M. L. Silverberg, M. A. Maloy, S. M. Devlin, C. L. Batlevi, G. L. Shah, M. Scordo, M. L. Palomba, P. B. Dahi, C. S. Sauter, B. D. Santomasso, E. Mead, M. A. Perales, DLBCL patients treated with CD19 CAR T cells experience a high burden of organ toxicities but low nonrelapse mortality. *Blood Adv.* **4**, 3024–3033 (2020).
10. K. Rejeski, A. Perez, P. Sesques, E. Hoster, C. Berger, L. Jentzsch, D. Mougiakakos, L. Frölich, J. Ackermann, V. Bücklein, V. Blumenberg, C. Schmidt, L. Jallades, B. Fehse, C. Faul, P. Karschnia, O. Weigert, M. Dreyling, F. L. Locke, M. von Bergwelt-Baildon, A. Mackensen, W. Bethge, F. Ayuk, E. Bachy, G. Salles, M. D. Jain, M. Subklewe, CAR-HEMATOTOX: A model for CAR T-cell–related hematologic toxicity in relapsed/refractory large B-cell lymphoma. *Blood* **138**, 2499–2513 (2021).
11. J. A. Hill, D. Li, K. A. Hay, M. L. Green, S. Cherian, X. Chen, S. R. Riddell, D. G. Maloney, M. Boeckh, C. J. Turtle, Infectious complications of CD19-targeted chimeric antigen receptor-modified T-cell immunotherapy. *Blood* **131**, 121–130 (2018).
12. K. Rejeski, W. G. Kunz, M. Rudelius, V. Bücklein, V. Blumenberg, C. Schmidt, P. Karschnia, F. Schöberl, K. Dimitriadis, L. von Baumgarten, J. Stemmler, O. Weigert, M. Dreyling, M. von Bergwelt-Baildon, M. Subklewe, Severe *Candida glabrata* pancolitis and fatal *Aspergillus fumigatus* pulmonary infection in the setting of bone marrow aplasia after CD19-directed CAR T-cell therapy—A case report. *BMC Infect. Dis.* **21**, 121 (2021).
13. K. Rejeski, A. Perez, G. Iacoboni, O. Penack, V. Bücklein, L. Jentzsch, D. Mougiakakos, G. Johnson, B. Arciola, C. Carpio, V. Blumenberg, E. Hoster, L. Bullinger, F. L. Locke, M. von Bergwelt-Baildon, A. Mackensen, W. Bethge, P. Barba, M. D. Jain, M. Subklewe, The CAR-HEMATOTOX risk-stratifies patients for severe infections and disease progression after CD19 CAR-T in R/R LBCL. *J. Immunother. Cancer* **10**, e004475 (2022).
14. L. J. Nastoupil, M. D. Jain, L. Feng, J. Y. Spiegel, A. Ghobadi, Y. Lin, S. Dahiya, M. Lunning, L. Lekakis, P. Reagan, O. Oluwole, J. McGuirk, A. Deol, A. R. Sehgal, A. Goy, B. T. Hill, K. Vu, C. Andreadis, J. Munoz, J. Westin, J. C. Chavez, A. Cashen, N. N. Bennani, A. P. Rapoport, J. M. Vose, D. B. Miklos, S. S. Neelapu, F. L. Locke, Standard-of-care axicabtagene ciloleucel for relapsed or refractory large B-cell lymphoma: Results from the US lymphoma CAR T consortium. *J. Clin. Oncol.* **38**, 3119–3128 (2020).
15. W. A. Bethge, P. Martus, M. Schmitt, U. Holtick, M. Subklewe, B. von Tresckow, F. Ayuk, E. M. Wagner-Drouet, G. G. Wulf, R. Marks, O. Penack, U. Schnetzke, C. Koenecke, M. von Bonin, M. Stelljes, B. Glass, C. D. Baldus, V. Vucinic, D. Mougiakakos, M. Topp, M. A. Fante, R. Schroers, L. Bayir, P. Borchmann, V. Buecklein, J. Hasenkamp, C. Hanoun, S. Thomas, D. W. Beelen, C. Lengerke, N. Kroeger, P. Dreger, GLA/DRST real-world outcome analysis of CAR-T cell therapies for large B-cell lymphoma in Germany. *Blood* **140**, 349–358 (2022).
16. S. Fried, A. Avigdor, B. Bielorai, A. Meir, M. J. Besser, J. Schachter, A. Shimoni, A. Nagler, A. Toren, E. Jacoby, Early and late hematologic toxicity following CD19 CAR-T cells. *Bone Marrow Transplant.* **54**, 1643–1650 (2019).
17. P. Godel, N. Sieg, J.-M. Heger, N. Kutsch, C. Herling, B.-N. Bärmann, C. Scheid, P. Borchmann, U. Holtick, Hematologic rescue of CAR T-cell-mediated prolonged pancytopenia using autologous peripheral blood hematopoietic stem cells in a lymphoma patient. *Hemasphere* **5**, e545 (2021).
18. K. Rejeski, Z. Wu, V. Blumenberg, W. G. Kunz, S. Müller, S. Kajigaya, S. Gao, V. L. Bücklein, L. Frölich, C. Schmidt, M. von Bergwelt-Baildon, X. Feng, N. S. Young, M. Subklewe, Oligoclonal T-cell expansion in a patient with bone marrow failure after CD19 CAR-T therapy for Richter-transformed DLBCL. *Blood* **140**, 2175–2179 (2022).
19. Q. Lin, X. Liu, L. Han, L. Liu, B. Fang, Q. Gao, Y. Song, Autologous hematopoietic stem cell infusion for sustained myelosuppression after BCMA-CAR-T therapy in patient with relapsed myeloma. *Bone Marrow Transplant.* **55**, 1203–1205 (2020).
20. K. Rejeski, A. Burchert, G. Iacoboni, P. Sesques, L. Fransecky, V. Bücklein, C. Trenker, R. Hernani, R. Naumann, J. Schäfer, V. Blumenberg, C. Schmidt, K. Sohlbach, M. von Bergwelt-Baildon, E. Bachy, P. Barba, M. Subklewe, Safety and feasibility of stem cell boost as a salvage therapy for severe hematotoxicity after CD19 CAR T-cell therapy. *Blood Adv.* **6**, 4719–4725 (2022).
21. K. Mullanfiroze, A. Lazareva, J. Chu, L. Williams, S. Burridge, J. Silva, R. Chiesa, K. Rao, G. Lucchini, S. Ghorashian, M. O'Reilly, B. Carpenter, V. Grandage, R. Hough, C. Roddie, P. J. Amrolia, CD34+-selected stem cell boost can safely improve cytopenias following CAR T-cell therapy. *Blood Adv.* **6**, 4715–4718 (2022).
22. K. Rejeski, R. Greco, F. Onida, I. Sánchez-Ortega, C. Bonini, A. Sureda, J. G. Gribben, I. Yakoub-Agha, M. Subklewe, An international survey on grading, diagnosis, and management of immune effector cell-associated hematotoxicity (ICAHT) following CAR T-cell therapy on behalf of the EBMT and EHA. *Hemasphere* **7**, e889 (2023).
23. N. Sharma, P. M. Reagan, J. L. Liesveld, Cytopenia after CAR-T cell therapy—A brief review of a complex problem. *Cancers (Basel)* **14**, 1501 (2022).
24. K. R. Juluri, Q. V. Wu, J. Voutsinas, J. Hou, A. V. Hirayama, E. Mullane, N. Miles, D. G. Maloney, C. J. Turtle, M. Bar, J. Gauthier, Severe cytokine release syndrome is associated with hematologic toxicity following CD19 CAR T-cell therapy. *Blood Adv.* **6**, 2055–2068 (2022).
25. M. D. Jain, H. Zhao, X. Wang, R. Atkins, M. Menges, K. Reid, K. Spitler, R. Faramand, C. Bachmeier, E. A. Dean, B. Cao, J. C. Chavez, B. Shah, A. Lazaryan, T. Nishihori, M. Hussaini, R. J. Gonzalez, J. E. Mullinax, P. C. Rodriguez, J. R. Conejo-Garcia, C. Anasetti, M. L. Davila, F. L. Locke, Tumor interferon signaling and suppressive myeloid cells are associated with CAR T-cell failure in large B-cell lymphoma. *Blood* **137**, 2621–2633 (2021).

26. F. L. Locke, J. M. Rossi, S. S. Neelapu, C. A. Jacobson, D. B. Miklos, A. Ghobadi, O. O. Oluwole, P. M. Reagan, L. J. Lekakis, Y. Lin, M. Sherman, M. Better, W. Y. Go, J. S. Wiezorek, A. Xue, A. Bot, Tumor burden, inflammation, and product attributes determine outcomes of axicabtagene ciloleucel in large B-cell lymphoma. *Blood Adv.* **4**, 4898–4911 (2020).
27. C. A. Dinarello, D. Novick, S. Kim, G. Kaplanski, Interleukin-18 and IL-18 binding protein. *Front. Immunol.* **4**, 289 (2013).
28. P. Y. Perera, J. H. Lichy, T. A. Waldmann, L. P. Perera, The role of interleukin-15 in inflammation and immune responses to infection: Implications for its therapeutic use. *Microbes Infect.* **14**, 247–261 (2012).
29. R. Faramand, M. Jain, V. Staedtke, H. Kotani, R. Bai, K. Reid, S. B. Lee, K. Spitler, X. Wang, B. Cao, J. Pinilla, A. Lazaryan, F. Khimani, B. Shah, J. C. Chavez, T. Nishihori, A. Mishra, J. Mullinax, R. Gonzalez, M. Hussaini, M. Dam, B. D. Brandjes, C. A. Bachmeier, C. Anasetti, F. L. Locke, M. L. Davila, Tumor microenvironment composition and severe cytokine release syndrome (CRS) influence toxicity in patients with large B-cell lymphoma treated with axicabtagene ciloleucel. *Clin. Cancer Res.* **26**, 4823–4831 (2020).
30. C. Gudiol, R. E. Lewis, P. Strati, D. P. Kontoyiannis, Chimeric antigen receptor T-cell therapy for the treatment of lymphoid malignancies: Is there an excess risk for infection? *Lancet Haematol.* **8**, e216–e228 (2021).
31. E. Bachy, S. Le Gouill, R. Di Blasi, P. Sesques, G. Manson, G. Cartron, D. Beauvais, L. Roulin, F. X. Gros, M. T. Rubio, P. Bories, J. O. Bay, C. C. Llorente, S. Choquet, R.-O. Casasnovas, M. Mohty, S. Guidez, M. Joris, M. Loschi, S. Carras, J. Abraham, A. Chauchet, L. D. La Rochelle, B. Deau-Fischer, O. Hermine, T. Gastinne, J. J. Tudesq, E. Gat, F. Broussais, C. Thieblemont, R. Houot, F. Morschhauser, A real-world comparison of tisagenlecleucel and axicabtagene ciloleucel CAR T cells in relapsed or refractory diffuse large B cell lymphoma. *Nat. Med.* **28**, 2145–2154 (2022).
32. T. Jain, A. Knezevic, M. Pennisi, Y. Chen, J. D. Ruiz, T. J. Purdon, S. M. Devlin, M. Smith, G. L. Shah, E. Halton, C. Diamonte, M. Scordo, C. S. Sauter, E. Mead, B. D. Santomasso, M. L. Palomba, C. W. Batlevi, M. A. Maloy, S. Giralt, E. Smith, R. Brentjens, J. H. Park, M.-A. Perales, S. Mailankody, Hematopoietic recovery in patients receiving chimeric antigen receptor T-cell therapy for hematologic malignancies. *Blood Adv.* **4**, 3776–3787 (2020).
33. K. Rejeski, Y. Wang, O. Albanyan, J. L. Munoz, P. Sesques, G. Iacoboni, L. L. Corral, R. Mohty, M. Dreyling, F. L. Locke, P. Barba, E. Bachy, Y. Lin, M. Subklewe, M. D. Jain, The CAR-HEMATOTOX score identifies patients at high risk for hematological toxicity, infections and poor clinical outcomes following brexucabtagene autoleucel in relapsed/refractory mantle cell lymphoma. *Blood* **140**, 651–653 (2022).
34. R. E. O'Neill, W. Du, H. Mohammadpour, E. Alqassim, J. Qiu, G. Chen, P. L. McCarthy, K. P. Lee, X. Cao, T cell-derived CD70 delivers an immune checkpoint function in inflammatory T cell responses. *J. Immunol.* **199**, 3700–3710 (2017).
35. M. Winkelmann, V. L. Bücklein, V. Blumenberg, K. Rejeski, M. Ruzicka, M. Unterrainer, C. Schmidt, F. J. Dekorsy, P. Bartenstein, J. Ricke, M. von Bergwelt-Baildon, M. Subklewe, W. G. Kunz, Lymphoma tumor burden before chimeric antigen receptor T-cell treatment: RECIL vs. Lugano vs. metabolic tumor assessment. *Front Oncol* **12**, 974029 (2022).
36. J. Veldman, Z. N. D. Alsada, A. Berg, W. J. Plattel, A. Diepstra, L. Visser, Soluble PD-L1 is a promising disease biomarker but does not reflect tissue expression in classic Hodgkin lymphoma. *Br. J. Haematol.* **193**, 506–514 (2021).
37. J. B. Mortensen, I. Monrad, M. B. Enemark, M. Ludvigsen, P. Kamper, M. Bjerre, F. d'Amore, Soluble programmed cell death protein 1 (sPD-1) and the soluble programmed cell death ligands 1 and 2 (sPD-L1 and sPD-L2) in lymphoid malignancies. *Eur. J. Haematol.* **107**, 81–91 (2021).
38. T. F. Rowley, A. al-Shamkhani, Stimulation by soluble CD70 promotes strong primary and secondary CD8+ cytotoxic T cell responses in vivo. *J. Immunol.* **172**, 6039–6046 (2004).
39. R. Yang, L. Sun, C. F. Li, Y. H. Wang, J. Yao, H. Li, M. Yan, W. C. Chang, J. M. Hsu, J. H. Cha, J. L. Hsu, C. W. Chou, X. Sun, Y. Deng, C. K. Chou, D. Yu, M. C. Hung, Galectin-9 interacts with PD-1 and TIM-3 to regulate T cell death and is a target for cancer immunotherapy. *Nat. Commun.* **12**, 832 (2021).
40. J. M. Logue, E. Zucchetti, C. A. Bachmeier, G. S. Krivenko, V. Larson, D. Ninh, G. Grillo, B. Cao, J. Kim, J. C. Chavez, A. Baluch, F. Khimani, A. Lazaryan, T. Nishihori, H. D. Liu, J. Pinilla-Ibarz, B. D. Shah, R. Faramand, A. E. Coghill, M. L. Davila, B. R. Dholaria, M. D. Jain, F. L. Locke, Immune reconstitution and associated infections following axicabtagene ciloleucel in relapsed or refractory large B-cell lymphoma. *Haematologica* **106**, 978–986 (2020).
41. J. H. Baird, D. J. Epstein, J. S. Tamaresis, Z. Ehlinger, J. Y. Spiegel, J. Craig, G. K. Claire, M. J. Frank, L. Muffly, P. Shiraz, E. Meyer, S. Arai, J. W. Brown, L. Johnston, R. Lowsky, R. S. Negrin, A. R. Rezvani, W. K. Weng, T. Latchford, B. Sahaf, C. L. Mackall, D. B. Miklos, S. Sidana, Immune reconstitution and infectious complications following axicabtagene ciloleucel therapy for large B-cell lymphoma. *Blood Adv.* **5**, 143–155 (2021).
42. R. D. Sandler, R. S. Tattersall, H. Schoemans, R. Greco, M. Badoglio, M. Labopin, T. Alexander, K. Kirgizov, M. Rovira, M. Saif, R. Saccardi, J. Delgado, Z. Peric, C. Koenecke, O. Penack, G. Basak, J. A. Snowden, Diagnosis and management of secondary HLH/MAS following HSCT and CAR-T cell therapy in adults; a review of the literature and a survey of practice within EBMT centres on behalf of the Autoimmune Diseases Working Party (ADWP) and Transplant Complications Working Party (TCWP). *Front. Immunol.* **11**, 524 (2020).
43. D. A. Lichtenstein, F. Schischlik, L. Shao, S. M. Steinberg, B. Yates, H. W. Wang, Y. Wang, J. Inglefield, A. Dulau-Florea, F. Ceppi, L. C. Hermida, K. Stringaris, K. Dunham, P. Homan, P. Jailwala, J. Mirazee, W. Robinson, K. M. Chisholm, C. Yuan, M. Stetler-Stevenson, A. K. Ombrello, J. Jin, T. J. Fry, N. Taylor, S. L. Highfill, P. Jin, R. A. Gardner, H. Shalabi, E. Ruppin, D. F. Stroncek, N. N. Shah, Characterization of HLH-like manifestations as a CRS variant in patients receiving CD22 CAR T cells. *Blood* **138**, 2469–2484 (2021).
44. E. S. Weiss, C. Girard-Guyonvarc'h, D. Holzinger, A. A. de Jesus, Z. Tariq, J. Picarsic, E. J. Schiffrin, D. Foell, A. A. Grom, S. Ammann, S. Ehl, T. Hoshino, R. Goldbach-Mansky, C. Gabay, S. W. Canna, Interleukin-18 diagnostically distinguishes and pathogenically promotes human and murine macrophage activation syndrome. *Blood* **131**, 1442–1455 (2018).
45. M. S. Zinter, M. L. Hermiston, Calming the storm in HLH. *Blood* **134**, 103–104 (2019).
46. K. Tamura, T. Kanazawa, S. Tsukada, T. Kobayashi, M. Kawamura, A. Morikawa, Increased serum monocyte chemoattractant protein-1, macrophage inflammatory protein-1beta, and interleukin-8 concentrations in hemophagocytic lymphohistiocytosis. *Pediatr. Blood Cancer* **51**, 662–668 (2008).
47. L. Lieben, Autoinflammatory diseases: Free IL-18 causes macrophage activation syndrome. *Nat. Rev. Rheumatol.*, (2018).
48. T. A. Fehniger, M. A. Caligiuri, Interleukin 15: Biology and relevance to human disease. *Blood* **97**, 14–32 (2001).
49. L. V. Hurton, H. Singh, A. M. Najjar, K. C. Switzer, T. Mi, S. Maiti, S. Olivares, B. Rabinovich, H. Huls, M. A. Forget, V. Datar, P. Kebriaei, D. A. Lee, R. E. Champlin, L. J. Cooper, Tethered IL-15 augments antitumor activity and promotes a stem-cell memory subset in tumor-specific T cells. *Proc. Natl. Acad. Sci. U.S.A.* **113**, E7788–E7797 (2016).
50. D. Alizadeh, R. A. Wong, X. Yang, D. Wang, J. R. Pecoraro, C. F. Kuo, B. Aguilar, Y. Qi, D. K. Ann, R. Starr, R. Urak, X. Wang, S. J. Forman, C. E. Brown, IL15 enhances CAR-T cell antitumor activity by reducing mTORC1 activity and preserving their stem cell memory phenotype. *Cancer Immunol. Res.* **7**, 759–772 (2019).
51. D. E. Morales-Mantilla, K. Y. King, The role of interferon-gamma in hematopoietic stem cell development, homeostasis, and disease. *Curr. Stem Cell Rep.* **4**, 264–271 (2018).
52. A. M. de Bruin, Ö. Demirel, B. Hooibrink, C. H. Brandts, M. A. Nolte, Interferon-γ impairs proliferation of hematopoietic stem cells in mice. *Blood* **121**, 3578–3585 (2013).
53. J. L. Benci, B. Xu, Y. Qiu, T. J. Wu, H. Dada, C. Twyman-Saint Victor, L. Cucolo, D. S. M. Lee, K. E. Pauken, A. C. Huang, T. C. Gangadhar, R. K. Amaravadi, L. M. Schuchter, M. D. Feldman, H. Ishwaran, R. H. Vonderheide, A. Maity, E. J. Wherry, A. J. Minn, Tumor interferon signaling regulates a multigenic resistance program to immune checkpoint blockade. *Cell* **167**, 1540–1554.e12 (2016).
54. J. L. Benci, L. R. Johnson, R. Choa, Y. Xu, J. Qiu, Z. Zhou, B. Xu, D. Ye, K. L. Nathanson, C. H. June, E. J. Wherry, N. R. Zhang, H. Ishwaran, M. D. Hellmann, J. D. Wolchok, T. Kambayashi, A. J. Minn, Opposing functions of interferon coordinate adaptive and innate immune responses to cancer immune checkpoint blockade. *Cell* **178**, 933–948.e14 (2019).
55. J. Qiu, B. Xu, D. Ye, D. Ren, S. Wang, J. L. Benci, Y. Xu, H. Ishwaran, J. C. Beltra, E. J. Wherry, J. Shi, A. J. Minn, Cancer cells resistant to immune checkpoint blockade acquire interferon-associated epigenetic memory to sustain T cell dysfunction. *Nat. Cancer* **4**, 43–61 (2023).
56. Y. Wang, Z. Song, Y. Geng, L. Gao, L. Xu, G. Tang, X. Ni, L. Chen, J. Chen, T. Wang, W. Fu, D. Feng, X. Yu, L. Wang, J. Yang, The risk factors and early predictive model of hematotoxicity after CD19 chimeric antigen receptor T cell therapy. *Front. Oncol.* **12**, 987965 (2022).
57. N. Tabbara, J. Sharp, D. Gaut, T. T. D. Pham, K. Tang, C. Oliai, M. S. Sim, G. Schiller, P. Young, J. P. Sasine, Diminished durability of chimeric antigen receptor T-cell efficacy with severe or prolonged postinfusion cytopenias. *Am. J. Hematol.* **97**, E249–E255 (2022).
58. M. L. Davila, C. C. Kloss, G. Gunset, M. Sadelain, CD19 CAR-targeted T cells induce long-term remission and B cell aplasia in an immunocompetent mouse model of B cell acute lymphoblastic leukemia. *PLOS ONE* **8**, e61338 (2013).
59. M. H. Kroll, C. Rojas-Hernandez, C. Yee, Hematologic complications of immune checkpoint inhibitors. *Blood* **139**, 3594–3604 (2022).
60. J. Wei, Y. Liu, C. Wang, Y. Zhang, C. Tong, G. Dai, W. Wang, J. E. J. Rasko, J. J. Melenhorst, W. Qian, A. Liang, W. Han, The model of cytokine release syndrome in CAR T-cell treatment for B-cell non-Hodgkin lymphoma. *Signal Transduct. Target. Ther.* **5**, 134 (2020).
61. K. Rejeski, D. K. Hansen, R. Bansal, P. Sesques, S. Ailawadhi, J. M. Logue, C. L. Freeman, M. Alsina, S. Theurich, F. L. Locke, E. Bachy, M. D. Jain, Y. Lin, M. Subklewe, The CAR-hematotox score as a prognostic model of toxicity and response in patients receiving BCMA-directed CAR-T for relapsed/refractory multiple myeloma. *Blood* **140**, 7506–7508 (2022).
62. M. D. Jain, B. Ziccheddu, C. A. Coughlin, R. Faramand, A. J. Griswold, K. M. Reid, M. Menges, Y. Zhang, L. Cen, X. Wang, M. Hussaini, O. Landgren, M. L. Davila, J. H. Schatz, F. L. Locke,

F. Maura, Whole-genome sequencing reveals complex genomic features underlying anti-CD19 CAR T-cell treatment failures in lymphoma. *Blood* **140**, 491–503 (2022).
63. K. Rejeski, M. D. Jain, E. L. Smith, Mechanisms of resistance and treatment of relapse after CAR T-cell therapy for large B-cell lymphoma and multiple myeloma. *Transplant. Cell. Ther.* **29**, 418–428 (2023).
64. H.-J. Cherng, R. Sun, B. Sugg, R. Irwin, H. Yang, C. C. Le, Q. Deng, L. Fayad, N. H. Fowler, S. Parmar, R. Steiner, F. Hagemeister, R. Nair, H. J. Lee, M. Rodriguez, F. Samaniego, S. P. Iyer, C. R. Flowers, L. Wang, L. J. Nastoupil, S. S. Neelapu, S. Ahmed, P. Strati, M. R. Green, J. Westin, Risk assessment with low-pass whole-genome sequencing of cell-free DNA before CD19 CAR T-cell therapy for large B-cell lymphoma. *Blood* **140**, 504–515 (2022).
65. C. J. Turtle, L. A. Hanafi, C. Berger, T. A. Gooley, S. Cherian, M. Hudecek, D. Sommermeyer, K. Melville, B. Pender, T. M. Budiarto, E. Robinson, N. N. Steevens, C. Chaney, L. Soma, X. Chen, C. Yeung, B. Wood, D. Li, J. Cao, S. Heimfeld, M. C. Jensen, S. R. Riddell, D. G. Maloney, CD19 CAR-T cells of defined CD4+:CD8+ composition in adult B cell ALL patients. *J. Clin. Invest.* **126**, 2123–2138 (2016).
66. K. Rejeski, D. M. Cordas Dos Santos, N. H. Parker, V. L. Bücklein, M. Winkelmann, K. S. Jhaveri, L. Liu, P. Trinkner, S. Günther, P. Karschnia, V. Blumenberg, C. Schmidt, W. G. Kunz, M. von Bergwelt-Baildon, M. D. Jain, S. Theurich, M. Subklewe, Influence of adipose tissue distribution, sarcopenia, and nutritional status on clinical outcomes after CD19 CAR T-cell therapy. *Cancer Immunol. Res.* **11**, 707–719 (2023).
67. D. W. Lee, B. D. Santomasso, F. L. Locke, A. Ghobadi, C. J. Turtle, J. N. Brudno, M. V. Maus, J. H. Park, E. Mead, S. Pavletic, W. Y. Go, L. Eldjerou, R. A. Gardner, N. Frey, K. J. Curran, K. Peggs, M. Pasquini, J. F. DiPersio, M. R. M. van den Brink, K. V. Komanduri, S. A. Grupp, S. S. Neelapu, ASTCT consensus grading for cytokine release syndrome and neurologic toxicity associated with immune effector cells. *Biol. Blood Marrow Transplant.* **25**, 625–638 (2019).
68. D. M. C. Dos Santos, K. Rejeski, M. Winkelmann, L. Liu, P. Trinkner, S. Günther, V. L. Bücklein, V. Blumenberg, C. Schmidt, W. G. Kunz, M. Von Bergwelt-Baildon, S. Theurich, M. Subklewe, Increased visceral fat distribution and body composition impact cytokine release syndrome onset and severity after CD19 chimeric antigen receptor T-cell therapy in advanced B-cell malignancies. *Haematologica* **107**, 2096–2107 (2022).
69. J.-A. H. Young, B. R. Logan, J. Wu, J. R. Wingard, D. J. Weisdorf, C. Mudrick, K. Knust, M. M. Horowitz, D. L. Confer, E. R. Dubberke, S. A. Pergam, F. M. Marty, L. M. Strasfeld, J. W. M. Brown, A. A. Langston, M. G. Schuster, D. R. Kaul, S. I. Martin, C. Anasetti; Blood and Marrow Transplant Clinical Trials Network Trial 0201, Infections after transplantation of bone marrow or peripheral blood stem cells from unrelated donors. *Biol. Blood Marrow Transplant.* **22**, 359–370 (2016).
70. B. D. Cheson, R. I. Fisher, S. F. Barrington, F. Cavalli, L. H. Schwartz, E. Zucca, T. A. Lister; Alliance, Australasian Leukaemia and Lymphoma Group; Eastern Cooperative Oncology Group; European Mantle Cell Lymphoma Consortium; Italian Lymphoma Foundation; European Organisation for Research; Treatment of Cancer/Dutch Hemato-Oncology Group; Grupo Español de Médula Ósea; German High-Grade Lymphoma Study Group; German Hodgkin's Study Group; Japanese Lymphorra Study Group; Lymphoma Study Association; NCIC Clinical Trials Group; Nordic Lymphoma Study Group; Southwest Oncology Group; United Kingdom National Cancer Research Institute, Recommendations for initial evaluation, staging, and response assessment of Hodgkin and non-Hodgkin lymphoma: The Lugano classification. *J. Clin. Oncol.* **32**, 3059–3068 (2014).
71. V. Blumenberg, S. Völkl, G. Busch, S. Baumann, M. Winkelmann, B. Tast, D. Nixdorf, G. Hänel, L. Frölich, C. Schmidt, R. Jitschin, F. Vettermann, W. Kunz, D. Mougiakakos, M. von Bergwelt, V. Bücklein, A. Mackensen, M. Subklewe, P04.01 immunomonitoring of CD19. CAR T-cells in large B-cell lymphoma—A two-center experience. *J. Immunother. Cancer* **9**, A16 (2021).
72. M. R. Filbin, A. Mehta, A. M. Schneider, K. R. Kays, J. R. Guess, M. Gentili, B. G. Fenyves, N. C. Charland, A. L. K. Gonye, I. Gushterova, H. K. Khanna, T. J. LaSalle, K. M. Lavin-Parsons, B. M. Lilley, C. L. Lodenstein, K. Manakongtreecheep, J. D. Margolin, B. N. McKaig, M. Rojas-Lopez, B. C. Russo, N. Sharma, J. Tantivit, M. F. Thomas, R. E. Gerszten, G. S. Heimberg, P. J. Hoover, D. J. Lieb, B. Lin, D. Ngo, K. Pelka, M. Reyes, C. S. Smillie, A. Waghray, T. E. Wood, A. S. Zajac, L. L. Jennings, I. Grundberg, R. P. Bhattacharyya, B. A. Parry, A. C. Villani, M. Sade-Feldman, N. Hacohen, M. B. Goldberg, Longitudinal proteomic analysis of severe COVID-19 reveals survival-associated signatures, tissue-specific cell death, and cell-cell interactions. *Cell Rep. Med.* **2**, 100287 (2021).
73. H. Nahi, M. Chrobok, S. Meinke, C. Gran, N. Marquardt, G. Afram, T. Sutlu, M. Gilljam, B. Stellan, A. K. Wagner, P. Blomberg, P. H. Holmqvist, L. Walther-Jallow, K. Mellström, J. Liwing, C. Gustafsson, R. Månsson, M. Klimkowska, G. Gahrton, J. Lund, P. Ljungman, H. G. Ljunggren, E. Alici, Autologous NK cells as consolidation therapy following stem cell transplantation in multiple myeloma. *Cell Rep. Med.* **3**, 100508 (2022).
74. K. Rejeski, V. Blumenberg, G. Iacoboni, L. Lopez-Corral, S. Kharboutli, R. Hernani, A. Petrera, N. Müller, F. Hildebrand, L. Frölich, P. Karschnia, C. Schmidt, D. M. Cordas dos Santos, J. L. Piñana, F. Müller, A. A. Martin, M. Dreyling, M. von Bergwelt-Baildon, P. Barba, M. Subklewe, V. L. Bücklein, Identifying early infections in the setting of CRS with routine and exploratory serum proteomics and the HT10 score following CD19 CAR-T for relapsed/refractory B-NHL. *Hemasphere* **7**, e858 (2023).

Acknowledgments: We are grateful for the support of all patients and the personnel who supported this work across all the participating centers. We would like to thank S. Forsberg from Olink Proteomics for the help with the bioinformatic analysis, as well as N. Müller (formerly Department of Medicine III, LMU Munich) for the support with the Olink experiments. We thank E. Habben, E. Zientara, B. Kirschbaum, and A. Kostrau (Laboratory for Leukemia Diagnostics, Flow Cytometry Unit, University Hospital, LMU Munich) for excellent technical support. We also acknowledge the iFlow Core Facility of the University Hospital, LMU Munich (INST 409/225-1 FUGG), and the Core Unit Cell Sorting and Immunmonitoring Erlangen (Florentine Schonath) for assistance with the generation of flow cytometry data. **Funding:** K.Rej. received a fellowship from the School of Oncology of the German Cancer Consortium (DKTK) and was funded by the Else Kröner Forschungskolleg (EKFK) within the Munich Clinician Scientist Program (MCSP). This work was supported by a grant within the Gilead Research Scholar Program (to K.Rej. and M.S.), the Bruno & Helene Jöster Foundation (to K.R., M.S.), and by a Deutsche Forschungsgemeinschaft (DFG, German Research Foundation) research grant provided within the Sonderforschungbereich SFB-TRR 338/1 2021 – 452881907 and DFG research grant 451580403 (to M.S.). The work was further supported by the Bavarian Elite Graduate Training Network (to M.S.), the Wilhelm-Sander Stiftung (to M.S., project no. 2018.087.1), the Else-Kröner-Fresenius Stiftung (to M.S.), and the Bavarian Cancer Research Center (BZKF). **Author contributions:** Conceptualization: K.Rej., M.D.J., and M.S. Investigation: K.Rej., A.Per., G.I., V.B., V.L.B., S.V., O.P., O.A., S.S., F.M., P.K., A.Pet., K.Rei., R.F., M.L.D., K.M., E.A.D., C.B., M.v.B.-B., F.L.L., W.B., L.B., A.M., P.B., M.D.J., and M.S. Formal analysis and visualization: K.Rej. Methodology: K.Rej., G.I., V.B., and V.L.B. Writing—original draft: K.Rej., M.D.J., and M.S. Writing—review and editing: K.Rej., A.Per., G.I., V.L.B., F.L.L., P.B., M.D.J., and M.S. All authors read and approved the final manuscript. **Competing interests:** K.Rej.: Kite/Gilead: Research funding and travel support; Novartis: Honoraria; BMS/Celgene: Consultancy and honoraria. A.Per.: Speaker's Bureau: Kite/Gilead, Curio. G.I.: Consultancy and honoraria: Novartis, Roche, Kite/Gilead, Bristol-Myers Squibb, Abbvie, Janssen, Sandoz, Miltenyi, and AstraZeneca. V.B.: Novartis: Honoraria and research funding; Gilead: Consultancy, honoraria, and research funding; BMS/Celgene: Research funding; Janssen: Honoraria and research funding; Roche: Research funding; Takeda: Research funding. V.L.B.: AMGEN: Honoraria; Celgene: Research funding; Pfizer: Honoraria; Kite/Gilead: Research funding and honoraria; Novartis: Honoraria. O.P. has received honoraria or travel support from Astellas, Gilead, Jazz, MSD, Neovii Biotech, Novartis, Pfizer, and Therakos. He has received research support from Gilead, Incyte, Jazz, Neovii Biotech, and Takeda. He is a member of advisory boards to Jazz, Gilead, MSD, Omeros, Priothera, Shionogi, and SOBI. F.M.: Novartis/Kite Gilead: Travel support and advisory/honoraria. R.F.: Novertis/Kite Gilead: Research support. M.L.D. reports research funding from Celgene, Novartis, and Atara; other financial support from Novartis, Precision Biosciences, Celyad, Bellicum, and GlaxoSmithKline; and stock options from Precision Biosciences, Adaptive, and Anixa. E.A.D. reports unlicensed patents (no royalties) held by the Moffitt Cancer Center that are unrelated to this work. M.v.B.-B.: Consultancy, research funding, and honoraria: MSD Sharp & Dohme, Novartis, Roche, Kite/Gilead, Bristol-Myers Squibb, Astellas, Mologen, and Miltenyi. F.L.L. has a scientific advisory role with Kite, a Gilead Company, Novartis, Celgene/Bristol-Myers Squibb, GammaDelta Therapeutics, Wugen, Amgen, Calibr, and Allogene; is a consultant with grant options for Cellular Biomedicine Group Inc.; receives research support from Kite, a Gilead Company, Novartis, and Allogene; and reports that his institution holds unlicensed patents in his name in the field of cellular immunotherapy. W.B.: Novartis: Consultancy, Honoraria; Gilead: Consultancy and honoraria; Miltenyi: Consultancy and research funding. L.B.: Advisory role or expert testimony: Abbvie, Bristol-Myers Squibb, Celgene, Daiichi Sankyo, Gilead, Hexal, Janssen, Jazz Pharmaceuticals, Menarini, Novartis, and Pfizer; Honoraria: Abbvie, Amgen, Astellas, Bristol-Myers Squibb, Celgene, Daiichi Sankyo, Janssen, Jazz Pharmaceuticals, Novartis, Pfizer, Sanofi, and Seattle Genetics; Financing of scientific research: Bayer and Jazz Pharmaceuticals. A.M.: Advisory and speaking engagement: Gilead and Novartis. P.B. declares having received honoraria from Allogene, Amgen, BMS, Jansen,Kite-Gilead, Incyte, Jazz Pharmaceuticals, Miltenyi Biomedicine, Novartis, and Nektar. M.D.J.: Kite/Gilead: Consultancy/Advisory; Novartis: Consultancy/Advisory; BMS/CELGENE: Consultancy/Advisory; Takeda: Consultancy/Advisory. M.S.: Morphosys: Research funding; Novartis: Consultancy and research funding; Janssen: Consultancy; Seattle Genetics: Research funding; AMGEN: Consultancy, honoraria, and research funding; Celgene: Consultancy and honoraria; Kite/Gilead: Consultancy, honoraria, and research funding; Roche AG: Consultancy and research funding. The remaining authors declare that they have no competing interests. None of the mentioned conflicts of interest were related to financing of the content of this manuscript. **Data and materials availability:** All data needed to evaluate the conclusions in the paper are present in the paper and/or the Supplementary Materials.

Submitted 20 December 2022
Accepted 23 August 2023
Published 22 September 2023
10.1126/sciadv.adg3919

ScienceAdvances

Severe hematotoxicity after CD19 CAR-T therapy is associated with suppressive immune dysregulation and limited CAR-T expansion

Kai Rejeski, Ariel Perez, Gloria Iacoboni, Viktoria Blumenberg, Veit L. Bücklein, Simon Völkl, Olaf Penack, Omar Albanyan, Sophia Stock, Fabian Müller, Philipp Karschnia, Agnese Petrera, Kayla Reid, Rawan Faramand, Marco L. Davila, Karnav Modi, Erin A. Dean, Christina Bachmeier, Michael von Bergwelt-Baildon, Frederick L Locke, Wolfgang Bethge, Lars Bullinger, Andreas Mackensen, Pere Barba, Michael D. Jain, and Marion Subklewe

Sci. Adv. **9** (38), eadg3919. DOI: 10.1126/sciadv.adg3919

Science Advances (ISSN 2375-2548) is published by the American Association for the Advancement of Science. 1200 New York Avenue NW, Washington, DC 20005. The title *Science Advances* is a registered trademark of AAAS.